

KERNFORSCHUNGSZENTRUM

KARLSRUHE

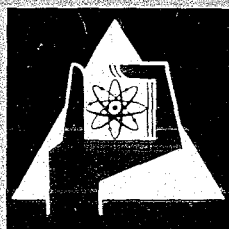
Mai 1969

KFK 1045
EUR 4311 e

Institut für Neutronenphysik und Reaktortechnik

The Influence of Nuclear Data Uncertainties of Reactor Materials
on the Main Safety and Stability Parameters of a Large
Steam-Cooled Fast Reactor (D-1 Design)

C.H.M. Broeders



GESELLSCHAFT FÜR KERNFORSCHUNG M. B. H.
KARLSRUHE



May 1969

KFK-1045
EUR 4311e

Institut für Neutronenphysik und Reaktortechnik

The Influence of Nuclear Data Uncertainties of Reactor
Materials on the main Safety and Stability Parameters
of a Large Steam-Cooled Fast Reactor (D-1 Design) *) **)

C.H.M. BROEDERS

- *) Work performed as final part of the study for electrical engineer
at the Eindhoven Technological University
- **) Work performed within the association in the field of fast reactors
between the European Atomic Energy Community and Gesellschaft für Kern-
forschung mbH., Karlsruhe.

Table of Contents

Introduction

1. The Reactor Considered and the Model for the Calculations.
2. The Reactor Parameters Considered.
3. The Methods Applied and the Computer Programs Used for the Investigations.
 - 3.1 The Calculation of the Reactor Parameters.
 - 3.2 Subdivision of the Energy Region.
 - 3.3 The Computer Programs Used.
4. The Uncertainties of the Cross Sections of the Materials in the Reactor Considered.
 - 4.1 Materials and Cross Sections Considered.
 - 4.2 Basic Group Constant Set.
 - 4.3 Sources of Information for the Evaluation of the Data Uncertainties.
 - 4.4 Evaluation of the Cross Section Uncertainties.
5. The Influence of the Data Uncertainties on the Reactor Parameters.
 - 5.1 Macroscopic Cross Section Variations.
 - 5.2 The Influence of the Data Uncertainties of the Reactor Materials.
6. The Influence of the Data Uncertainties on the Safety, Stability and Dynamic Behaviour of the D-1 Design.
 - 6.1 The Uncertainties of the Most Important Parameters.
 - 6.2 The Influence on the Safety.
 - 6.3 The Stability of the Core.
 - 6.4 The Stability of the Plant.
 - 6.5 The Dynamic Behaviour of the Core.
7. Conclusions.

List of Figures.

References.

Introduction

Investigation of the D-1 design for a 1,000 MWe steam-cooled fast breeder reactor showed that the D-1 design is near the boundary of inherent stability. Within the expected uncertainties of the feedback coefficients the core may become unstable. In earlier studies, mainly on sodium-cooled fast breeder reactors, it was found that the feedback coefficients are rather sensitive to the nuclear data uncertainties. Therefore, in this study the influence of the nuclear data uncertainties on the main parameters for the safety and stability of the D-1 design are primarily investigated. These parameters are the Doppler coefficient and the steam-density coefficient. Moreover, the influence of the data uncertainties on the loss of coolant reactivity, the conversion ratio of the core and the amount of fissile material required is considered. Mainly the influence of the uncertainties of the capture and fission cross-sections is examined. Only for the materials U^{238} and Pu^{239} the influence of the inelastic cross-section uncertainties is considered too. Most investigations were performed with the help of multi-group diffusion calculations in a fundamental mode approximation. For these calculations the KFK-SNEAK set was used as basic group constant set. After each cross-section variation the reactor parameters considered were calculated for a critical reactor. In order to obtain some general information about the influence of the nuclear data uncertainties on the Doppler coefficient and the steam-density coefficient, the effect on these parameters following a 10% increase in the macroscopic cross-sections for capture and fission are first investigated. After that the influence of the data uncertainties of the reactor materials are calculated. Moreover, for the Doppler effect the results of different calculation methods are compared.

In the last chapter the influence of the reactor parameter uncertainties (found in this study) on safety, stability and dynamic behaviour of the D-1 design is investigated.

1. The Reactor Considered and the Model for the Calculations.

The study is performed for the D-1 design for a large steam-cooled fast breeder reactor which is the first detailed design for a 1,000 MWe reactor of this type undertaken by the Kernforschungszentrum Karlsruhe. The design is based on the $U^{238} - Pu^{239}$ cycle and is described in detail elsewhere [1,2]. It was pointed out that the D-1 design does not claim to be the optimum of possible steam-cooled breeder reactors. The intention was that extensive analyses would lead to a more optimal design.

The D-1 design has a cylindrical core with H/D ratio 0.575. The core is subdivided in 7 zones (Fig. 1). The 2 fission core zones have a different ratio of the fertile to the fissile material in a way that the maximum power densities in these parts are about the same.

Most calculations are performed with a fundamental mode multi-group diffusion approximation using the same buckling for all energy groups. This geometrical buckling was calculated with the formula

$$B_g^2 = \left(\frac{\pi}{H_c + 2S} \right)^2 + \left(\frac{2.405}{R_c + S} \right)^2 \quad (1.1)$$

H_c height of the unreflected core.

R_c radius of the unreflected core.

S effective saving.

The saving is determined by comparison of fundamental mode calculations with more detailed calculations for the reflected system. For the D-1 core the saving is about 16 cm.

$$B_g^2 = \underline{5.69 \cdot 10^{-4}} \text{ cm}^{-2}$$

The calculations are performed at maximum burn-up. It is assumed that in this case no control rod materials are in the core but the control rod followers of Al_2O_3 .

For the homogenized core the design parameters are collected in table 1.1.

Description	Material	Volume fraction
Fuel	PuO ₂ -UO ₂	0.454
Cladding + Structure	Inconel 625	0.206
Coolant	H ₂ O steam	0.32
Control rod follower	Al ₂ O ₃	0.02

Table 1.1.

The fuel density is assumed to be 0.87 of the theoretical values. The normal mean steam density is $\rho = 0.0706 \text{ g/cm}^3$ ($\approx 170 \text{ ata} \approx 2600 \text{ p.s.i.}$).

The isotopic composition of the Plutonium after a number of fuel recyclings is nearly constant [3,4,7]. For the D-1 design the core and the blanket material will be treated together. In this case the Plutonium composition becomes [5,7]:

Pu²³⁹ 74%; Pu²⁴⁰ 22.7%; Pu²⁴¹ 2.3%; Pu²⁴² 1.0%.

The maximum burn-up is 55.000 MWd/t being equivalent with 3.45% atom burn-up.

With these parameters and the group cross-section constants of the KFK-SNEAK set [7] the homogenized core is just critical at 900°K with the following atom-densities (table 1.2.)

Material	Atom-density 10 ²⁴ cm ⁻³	Material	Atom-density 10 ²⁴ cm ⁻³
Al	7.34 10 ⁻⁴	O	2.12903 10 ⁻²
Cr	4.42974 10 ⁻³	Pu ²³⁹	1.12238 10 ⁻³
Fe	5.62485 10 ⁻⁴	Pu ²⁴⁰	3.44298 10 ⁻⁴
H	1.49785 10 ⁻³	Pu ²⁴¹	3.48849 10 ⁻⁵
Mo	9.82257 10 ⁻⁴	Pu ²⁴²	1.51673 10 ⁻⁵
Nb	4.50843 10 ⁻⁴	U ²³⁸	7.86809 10 ⁻³
Ni	1.10588 10 ⁻²	pairs of fission products	3.35346 10 ⁻⁴

Table 1.2.

In figure 2 the neutron flux distribution for the steam-densities $\rho = 0$ and $\rho = 0.0706$ is plotted. Figure 12 shows the adjoint flux. Figure 4,5 and 6 give the energy dependence of the capture and fission rates of the most important reactor materials.

x)

Some reactor parameters are

Loss of coolant reactivity	ΔK_L	= $3.64 \cdot 10^{-2}$	
Reduced steam-density coefficient R.S.D.C.		= $-2.14 \cdot 10^{-2}$	at 900°K
Conversion ratio	C.R.	= 0.9857	
Doppler constant	A_D	= $-1.386 \cdot 10^{-2}$	

2. The Reactor Parameters Considered.

The most important coefficient for the safety and stability of a fast steam-cooled reactor are the Doppler coefficient and the steam-density coefficient since they form the largest feedback reactivity effects. In a large fast reactor the Doppler coefficient is a prompt negative reactivity effect [9]. Because of the small neutron life-times in fast reactors this prompt negative reactivity is important for the control and safety of the reactor. In [29] it is shown that large steam-cooled fast reactors are inherent stable only if the steam-density coefficient is negative and if its absolute value is not too large. For the safety of the reactor also the loss of coolant reactivity is important because it is a significant value for the reactivity ramp after large disturbances in the cooling system. With the calculation methods applied also the ratio of the fertile to the fissile material and the conversion ratio of the core could be easily determined.

x) For the description of these parameters see chapters 2 and 3.

Therefore, the following parameters are considered:

- 1) Doppler coefficient
- 2) Steam-density coefficient
- 3) Loss of coolant reactivity
- 4) Ratio of the fertile to the fissile material
- 5) Conversion ratio of the core.

3. The Methods Applied and the Computer Programs Used for the Investigations.

For the selection of the calculation methods the following considerations were important:

- a) The influence of the data uncertainties on the reactor parameters should be calculated for critical reactors. After every cross-section variation the reactor should be made critical again.
- b) The investigations should be done with existing programs if possible.
- c) The computing times required should be as moderate as possible.

The calculations were performed with the IBM 7074 digital computer situated at the Kernforschungszentrum Karlsruhe. For the investigations of the influence of the data uncertainties on the reactor parameters computer programs developed by members of the Institut für Neutronenphysik und Reaktortechnik were used. Most of these programs are collected in the "Nuclear code system NUSYS" [10]. The influence of the parameter variations on the stability and dynamic behaviour of the reactor (described in chapter 6) was investigated with programs developed by members of the Institut für Reaktorentwicklung.

3.1. The calculation of the reactor parameters.

3.1.1. The Doppler Coefficient D.C.

For the calculation of the Doppler Coefficient $D.C. = \frac{dK}{dT}$ two calculation methods were considered:

- a) The method of Nicholson-Froelich [11,12]. The D.C. is calculated directly in a perturbation calculation with the help of the temperature derivatives of the capture and fission cross sections of the fuel isotopes.
- b) Method of successive K-calculation. The multiplication factor K of the reactor system is calculated for several temperatures. With the help of a temperature law for the D.C. the latter may be determined.

Both methods have some advantages and disadvantages for the present study:

- With method a) the D.C. is calculated directly. At the Kernforschungszentrum Karlsruhe Froelich and Siep have developed a Computer Code [13] based on the theory of KFK 367 [12]. Because the resonances are described by the statistical distributions of the resonance parameters, the results only are sufficient accurate if the number of resonances in an energy group is sufficient large. Therefore, the D.C. is only calculated in the energy range $100 \text{ eV} < E < 100 \text{ KeV}$. For sodium cooled fast breeder reactors the lower energy limit only introduces small cross [5]. However, for steam cooled fast reactors with a considerable weaker neutron spectrum the contribution of the energy region below 100 eV may be significant.
- With method b) the whole energy region is considered. Here the trouble is introduced by the temperature law for the D.C. Usually the following dependence is applied:

$$\text{D.C.} = \frac{dK}{dT} = \frac{a}{T^x} \quad (3.1)$$

With the help of 3 values of K at different temperatures the constants a and x may be determined.

Often it is assumed that the D.C. is inverse proportional to the absolute temperature (x = 1). In this case:

$$\text{D.C.} = \frac{dK}{dT} = \frac{A_D}{T} \quad (3.2)$$

The constant A_D may be determined with the help of K at 2 temperatures:

$$A_D = \frac{K(T_1) - K(T_2)}{\ln T_2/T_1} \quad (3.3)$$

- If in the resonance region the group constants change, the resonance parameters have to change too. With both methods a) and b) it is difficult to take into account these resonance parameter variations. In method a) a tape with fixed resonance parameters has to be changed while in method b) the selfshielding factors for the group constants should be changed.

It was decided to calculate the multiplication factor of the system at two temperatures ($T_1 = 900^\circ\text{K}$ and $T_2 = 2100^\circ\text{K}$) and to apply the temperature law of formula (3.2). The Doppler constant A_D may be calculated with formula (3.3). The reasons for this selection are:

- a) For the higher Pu isotopes the Karlsruhe GROUCO file only contains selfshielding factors at 2 temperatures.
- b) With the method selected the effects of the whole energy region are considered .
- c) For cross section variations in the resonance energy region the variation of the resonance parameters is not considered explicitly. It is expected that the resonance parameters have less influence on the temperature dependence of the selfshielding factors than on the temperature derivatives of the cross sections. The errors introduced will be smaller for the method selected than for the method of Nicholson-Froelich.

3.1.2. The reduced steam density coefficient R.S.D.C.

The R.S.D.C. is defined by:

$$\text{R.S.D.C.} = \frac{dK}{K} / \frac{d\rho}{\rho} \quad \text{at normal steam density} \quad (3.4)$$

The following approximation is applied:

$$\text{R.S.D.C.} = \frac{\rho_N}{K} \frac{\{K(\rho_N + \delta\rho) - K(\rho_N)\}}{2\delta\rho} \quad (3.5)$$

with $\delta\rho = 0.01 \rho_N$

3.1.3. The loss of coolant reactivity

$$\Delta K_L = K(\rho = 0) - K(\rho = \rho_N) \quad (3.6)$$

The multiplication factor $K(\rho = 0)$ and $K(\rho = \rho_N)$ are calculated with the same group constant set (KFK-SNEAK /6,7,7). Because the neutron flux spectrum is varying considerably if the steam density varies between $\rho = \rho_N$ and $\rho = 0$, group constant sets with different weighting spectra are required in order to calculate ΔK_L accurate. However, it may be expected that the influence of the nuclear data uncertainties may be investigated rather well with one group constant set.

3.1.4. The conversion ratio of the core.

With the fundamental mode calculations the conversion ratio of the core is approximated by the ratio of the captures per volume unit in the fertile material to the absorptions per volume unit in the fissile material.

3.2. Subdivision of the energy region

The effects of variation of several cross sections of several materials have to be considered. The calculations are performed with multi-group calculations using 26 groups. Each of the group constants has an uncertainty and also a certain effect on the parameters considered. With the calculation methods applied it was impossible to consider the effect of each group constant separately. So a suitable subdivision of the energy region was necessary. This subdivision of the energy spectrum was based on properties of the nuclear data and of the system observed. Moreover, during the calculations it seemed that some subdivisions should be performed or could be omitted.

The following properties were considered:

3.2.1. Nuclear data

3.2.1.1. In different energy regions certain processes are dominant.

For an isotope with resonances, for example

- a) region below resonances
- b) region with resolved resonances
- c) region with unresolved (statistical) resonances
 - weakly overlapping resonances
 - considerably overlapping resonances
 - strongly overlapping resonances
- d) region above resonances
(the resonance effect is not noticeable any more)

3.2.1.2 In different energy regions the nuclear data are determined by different methods or experimental groups or laboratories. In this case attention should be paid to determine systematical errors.

3.2.2. The system observed

With respect to the energy spectrum subdivision important properties of the system are:

- a) The energy spectrum of the flux and of the adjoint flux (figures 2,12).
- b) The energy dependence of the most important reaction rates (figures 3,4,5).

In this study most attention is paid to the D.C. and to the R.S.D.C. So, analyses of these parameters may give important information too. Figures 6 and 7 show the energy dependence of these parameters.

The investigations have started with the following energy spectrum subdivision:

- 1) $1.4 \text{ MeV} < E < 10.5 \text{ MeV}$ or group 1 to 4,
because
 - a) energy region above resonances
 - b) main energy region of the fission neutrons
 - c) decreasing flux and reaction rates.

- 2) $46.5 \text{ keV} < E < 1.4 \text{ MeV}$ or group 5 to 9,
because
- a) flux and reaction rates at maximum
 - b) most influence on the Doppler effect below 46.5 keV
 - c) energy dependent contributions to the R.S.D.C. change sign between group 9 and 10 (figure 7).
- 3) $46.5 \text{ eV} < E < 46.5 \text{ keV}$ or group 10 to 18,
because
- a) main energy region for the Doppler effect
 - b) region with large uncertainties in σ_γ of Pu^{239}
 - c) flux and reaction rates still large.

More detailed calculations showed that in this energy range the groups 15 to 18 were dominant for the influence on the R.S.D.C.

Therefore, this region was further divided.

3-A $1 \text{ keV} < E < 46.5 \text{ keV}$ or group 10 to 14

3-B $46.5 \text{ eV} < E < 1 \text{ keV}$ or group 15 to 18

- 4) $E < 46.5 \text{ eV}$ or group 19 to 26,
because
- a) below main region for the Doppler effect
 - b) in this energy range the flux and reaction rates are relatively small.

For the materials U^{238} and Pu^{239} the energy region 46.5 eV to 46.5 keV (group 10 to 18) was examined more extensively. For the less important materials the subdivision of the energy spectrum was kept less detailed.

3.3. The Computer Programs Used.

3.3.1. The Calculation of the Reactor Parameters.

For the investigation of the influence of the cross section uncertainties on the reactor parameters mainly the multiplication factor K for different states of the reactor is to be calculated. The latter was

done with programs of the NUSYS system [10]. Program 446 by Sanitz enables the calculation of the macroscopic cross sections of the system taking into account the self-shielding effect. The multiplication factor in the fundamental mode approximation was calculated with program 352 by Ferranti and Kraetsch giving K with a truncation error of 10^{-6} . Some calculations with one-dimensional approximation of the diffusion equation were done with program 6731 by Sanitz and Woll. After each variation in the group constant set the reactor was made critical by variation of the ratio γ (fertile to fissile material). This was done with the iteration program 2210 by Bachmann. For the determination of the conversion ratio of the core the evaluation program 447 by Sanitz was used.

3.3.2. The variation of the group constant set.

If a group cross-section changes several other group constants may change too (e.g. Σ_f^i variation influences also $\nu\Sigma_f^i$, Σ_{rem}^i and Σ_{tr}^i). In order to maintain the relations between the group constants 2 programs were available:

a) NUSYS program 4840 by Langner.

In this program all group constants are modified except for $K\Sigma_{tr}$. The possibility for changing the latter is available separately.

For each NUSYS run the group constants have to be modified again.

b) Program 2229 by Bachmann.

With this program a new tape with group constants is arranged.

Both group constants for infinite dilution and self-shielding factors for the removal and transport cross-sections are modified.

The main difference between the 2 programs is the treatment of Σ_{tr} . Indeed, the determination of Σ_{tr} for the multi-group diffusion calculations is not well defined because of the weighting procedure. Moreover, variation of Σ_f and Σ_γ between extreme limits may introduce Σ_t variations out of the uncertainty range of the latter if the balance

$$\Sigma_t = \Sigma_\gamma + \Sigma_f + \Sigma_{in} + \Sigma_e$$

is maintained.

Comparison of the methods showed only very small differences in the parameters considered. Mainly for reasons of computing time required the second method by Bachmann is being used for most calculations. The variation of the total macroscopic cross-sections was done with MUSYS program 4837 by Langner. The latter has the same features as program 4840.

4. The Uncertainties of the Cross Sections of the Materials in the Reactor Considered.

4.1. Materials and Cross Sections Considered

4.1.1. Materials

The D-1 design includes the following materials

Fuel: PuO_2 and UO_2 with the following isotopes

Pu^{239} , Pu^{240} , Pu^{241} , Pu^{242} , U^{238} and in a very small amount U^{235} .

Structural materials: Cr, Fe, Mo, Nb, Ni and in a small amount Al.

Coolant: Light water steam: H_2O .

Also the fission products of Pu^{239} are considered.

Al and U^{235} will not be considered here because of the very small amounts.

4.1.2. Cross Sections

From similar studies on sodium-cooled reactors [14,15] it may be expected that the most important influence will be due to capture and fission cross section uncertainties. Moreover, in this chapter the uncertainties of the total inelastic scattering cross sections and of ν for Pu^{239} will be considered. Not considered are the uncertainties of the resonance parameters of the fuel materials. The latter may be important for the Doppler coefficient calculations with the help of the method of Froelich.

4.2. Basic Group Constant Set

As basic group constant set the KFK-SNEAK set was used. The energy spectrum is divided into 26 groups. The group boundaries are the same as in the Russian ABN set [8]. For some less important materials the group constants of the KFK-SNEAK set are taken from the ABN set.

The KFK-SNEAK set was chosen for the following reasons:

- a) Recent nuclear data are incorporated for the most important reactor materials.
- b) For the calculation of the group constants the expected neutron energy spectrum of a steam-cooled fast reactor is used, namely the calculated spectrum of the SNEAK 3A-2 core with an equivalent steam-density as in the large reactor ($\rho = 0.07 \text{ g/cm}^3$) [7].

4.3. Sources of Information for the Evaluation of the Data Uncertainties.

The basic source of information was KFK 120 part I by J.J. Schmidt [16]. For the higher Pu isotopes and the structural material Nb, in this reference no data are available. Here, BNL 325 second edition [17] and evaluations by Yiftah et al [18] and Pitterle et al. [19] were used. In addition for some materials recent publications were considered.

- a) For Pu^{239} the effect of recent α -measurements by Schomberg et al. [20]. The latter result in remarkable uncertainties of α and σ_γ in the energy region 0.5 keV to 30 keV.
- b) For Pu^{239} the effect of recent σ_f data for U^{235} by Beckurts et al. [21] on the normalization of σ_f measurements for Pu^{239} by White et al. [22] in the energy region 40 keV to 500 keV.
- c) For U^{238} the effect of σ_γ measurements by Pönitz et al. [23].

4.4. Evaluation of the Cross Section Uncertainties.

4.4.1. Pu^{239}

Pu^{239} is the main fissile material of the D-1 design. However, due to the lack of measurements and to systematic deviations in available data the cross sections of this material still have rather large uncertainties. Moreover, recently some experimental data were reported considerably deviating from the formerly recommended values

- a) Arnold et al. [24] reported for a steam cooled fast reactor lattice, with an energy spectrum similar to the spectrum of the D-1 design (figure 8) a mean value for α

$$\bar{\alpha} = \frac{\langle \sigma_{\gamma} \rangle}{\langle \sigma_f \rangle} = 0.57 \pm 0.13$$

being significant larger than the calculated value $\bar{\alpha} = 0.3873$.

As comparison, calculations for the D-1 design give

- with the ABN set $\bar{\alpha} = 0.329$

- with the KFK-SNEAK set $\bar{\alpha} = 0.325$

- b) Schomberg et al. [20] found with a new experimental method much larger values of α in the energy region 0.5 keV to 50 keV (preliminary results not corrected for multiple scattering).

The results of Schomberg et al. are taken into account in the following way (figure 9):

Because these preliminary results are probably too high as upper limit in α an average curve through the experimental values is chosen instead of a curve through the upper uncertainty limits of the measurements.

Since the true α -values in this energy region are very probably higher than the α -values of the KFK-SNEAK set the latter are chosen as lower limits.

The uncertainty of σ_{γ} is obtained by combining the uncertainties of σ_f and α because σ_{γ} is to be calculated indirectly from σ_f and α -measurements. Large uncertainties result in the energy region 0.5 keV to 50 keV.

The uncertainties of σ_f are mainly taken from KFK 120-I with one complication in the energy region 30 keV to 500 keV.

In this region the SNEAK set contains the data of White et al. [22] being considerably lower than the recommended values in KFK 120/I. As upper uncertainty limit the upper limits of σ_f in KFK 120/I are chosen. The lower limit of the uncertainties is obtained by the following renormalization of the White data:

The σ_f measurement for Pu^{239} of White is relative to the σ_f of U^{235} . White has calculated $^{49}\sigma_f$ *) with the help of his values for $^{25}\sigma_f$. Recently, Beckurts [21] has recommended new, smaller values of $^{25}\sigma_f$. These smaller values lead to smaller values of $^{49}\sigma_f$.

*) The left upper index 49 comes from $^{94}\text{Pu}^{239}$, 25 from $^{92}\text{U}^{235}$ etc.

For energy regions not mentioned, the uncertainty estimations of KFK 120/I are taken. This also was done for the inelastic cross section.

The estimated uncertainties are collected in table 4.1.

4.4.2. U²³⁸

U²³⁸ is the main fertile material in the reactor. As may be seen in figure 4 an important part of the captures is due to U²³⁸. Moreover, in the energy region above 1.4 MeV the number of fissions of U²³⁸ is relatively large (figure 5).

The SNEAK set group constants are calculated with the last recommended data of KFK 120/I. In estimating the uncertainties only one more recent measurement of σ_γ by Pönitz et al. [23] in the energy region 25 keV - 500 keV had to be considered.

Between 40 keV and 200 keV KFK 120/I ascribes an uncertainty range of 20-30% for σ_γ . The Pönitz measurements are altogether within the lower uncertainty limit of 20%. Therefore, it appears to be reasonable to assume an uncertainty of 20% in this region.

For other energies the (mean) values of the KFK 120/I uncertainties are taken. The uncertainties collected are given in table 4.2.

4.4.3. Structural Materials

Figure 4 shows the capture rates for the structural materials. The latter are of the order of 1-10% of the U²³⁸ capture rates except for Fe with smaller values. However, Ni has more dominating capture rates in the upper and lower energy regions.

The SNEAK group constants are obtained in the following way.

- Cr, Fe and Ni are calculated with the data of KFK 120/I
- Mo and Nb have the existing group constants of the ABN set.

For the structural materials no more important recent measurements became available in excess of those already considered in KFK 120/I.

So, the given uncertainty values of KFK 120-I are taken over unchanged for Ni, Fe and Cr. For Mo and Nb the ABN data are compared with the data of KFK 120/I.

The missing uncertainty estimates for Fe in the energy range 2 keV to 100 keV and for Ni in the region 1 keV to 200 keV are obtained by crude estimation from available data in KFK 120/I.

Above 1 MeV the capture of Ni and Fe is mainly due to (n,p) processes. So, the tabulated uncertainty values are those of $\sigma(n,p)$. For Cr the $\sigma(n,p)$ and σ_γ have about the same order of magnitude above 1 MeV. However, only a few information about $\sigma(n,p)$ is available. Therefore, the expected maximum uncertainty values for σ_γ are tabulated.

For Nb the uncertainties are determined by comparing the ABN and BNL 325 data.

Capture Nb

~~Above 1 MeV only few BNL 325 data are given. However, the capture cross-sections in this region are very small. An arbitrary uncertainty of 20% is tabulated.~~

In the energy region 10 keV - 1 MeV comparison between ABN and BNL 325 data is possible. The ABN data are systematically somewhat higher. The upper and lower limits for the BNL 325 data are obtained by curves through the extreme values of the plotted measurements. Below 1 keV a comparison between ABN and BNL 325 data is difficult because BNL 325 gives resolved resonance parameters and the ABN data are group constants. Again, an arbitrary uncertainty of 15% is chosen.

Below the first resonance at 35.8 eV the uncertainty is equal to the uncertainty at thermal energy being $\pm 5\%$.

Inelastic scattering Nb

Comparison of BNL 325 and ABN data in the energy region below 2.5 MeV only shows a significant deviation in group 4 (1.4 MeV to 2.5 MeV). The $\pm 15\%$ uncertainty of BNL 325 in this region is tabulated. In group 4

the ABN value is compared with the BNL 325 limits.

Above 2.5 MeV no comparison is possible. An arbitrary uncertainty of 10% is tabulated because at these high energies the inelastic scattering cross sections generally are rather accurate.

The uncertainties collected for the structural materials are given in tables 4.3, 4.4 and 4.5.

4.4.4. Higher Pu Isotopes

In KFK 120/I no data for the higher Pu isotopes were considered. The SNEAK set contains the same group constants as the ABN set. The uncertainty evaluation is done with the help of BNL 325 [17] and of evaluations of Yiftah et al. [18] and Pitterle et al. [19]. For energies below 1 keV only resonance parameters with uncertainties are available what means that comparison of the recommended data with the ABN data is difficult.

Above 1 keV in the papers of Yiftah and Pitterle curves for fission and capture cross sections are given. Here the comparison between these data and the ABN data is easier to do.

Because there are less measurements for the higher Pu isotopes a reasonable estimation for the uncertainties of the group constants calculated from resonance data seems to be:

- + 15% below 1 keV
- + 25% for group constants calculated with
resonance parameters for energies above 1 keV

For energies above 1 keV, the evaluation is done per isotope.

4.4.4.1. Pu²⁴⁰

Pu²⁴⁰ may be considered to be the most important higher Pu isotope. Several studies indicate its influence on safety coefficients, e.g. the recent studies of Kiefhaber [25] and Jirlow [26].

Yet, the difference between the ABN and the recent evaluation of Yiftah et al. and Pitterle et al. are considerable.

Figure 10 shows the evaluations of Yiftah, Pitterle and the ABN group constants.

As upper and lower limits for the group constants are determined

a) Capture

In the energy region $E \geq 1$ keV

upper limit: the ABN data

lower limit: the modified ENDF-B data of Pitterle

In the energy region below 1 keV

upper limit: the ABN data

lower limit: the ABN data minus 30%

The latter is chosen since at 1 keV the modified ENDF/B value is about 30% smaller than the ABN value.

b) Fission

Above 465 keV the uncertainty bars in the paper of Yiftah are used for the determination of the upper and lower limits for the uncertainty.

In the energy region $10 \text{ keV} < E < 465 \text{ keV} \pm 20\%$ uncertainty in the data of Yiftah is assumed. Below 10 keV the modified ENDF/B and the ENDF/B data of Pitterle are used as upper and lower limits respectively. For the average number of neutrons per fission $\bar{\nu}$ the expression of Yiftah was used:

$$\bar{\nu} = 3.00 + 0.101 E \quad E \text{ in MeV}$$

The upper and lower limits for the group constants are tabulated in table 4.6.

4.4.4.2. Pu²⁴¹

a) Capture

The capture cross section data of Yiftah are partly (1 keV $\leq E < 50$ keV) calculated from resonance parameters and partly taken equal to σ_{γ} of Pu²³⁹ ($E < 50$ keV) because of the convergence of $^{49}\sigma_{\gamma}$ and $^{41}\sigma_{\gamma}$ below 50 keV.

However, it is very difficult to estimate reliable uncertainties

for this evaluation particularly because of the large uncertainties of $^{49}\sigma_{\gamma}$.

The differences between ABN and Yiftah data are not significant. Only at the highest energies (the first energy groups) the cross sections differ by a factor of about 2 (ABN larger). However, here the cross sections are very small.

The uncertainty of the Yiftah data is estimated to be 30%. The uncertainties of the ABN data are obtained by comparing with the Yiftah limits.

b) Fission

The fission cross-section data of Yiftah are based on the evaluation of Davey [27]. The uncertainties estimated by Davey are

1 keV < E < 40 keV	15%
40 keV < E < 10 MeV	10%

~~These values were considered as upper and lower limits for the Yiftah data. The uncertainty of the ABN data is obtained by comparing the latter with the limits of the Yiftah data.~~

Rather large deviations exist between ABN and Yiftah data.

1 keV < E < 100 keV	ABN data 20-30% larger
500 keV < E < 10 MeV	ABN data 20-30% smaller

The estimated uncertainties are collected in Table 4.6.

4.4.4.3. Pu²⁴²

a) Capture

The capture data of Yiftah in the energy region 1 keV < E < 1 MeV are calculated from the resonance parameters. This curve converges with increasing energy to the $^{28}\sigma_{\gamma}$ curve.

Above 1 MeV, $^{42}\sigma_{\gamma}$ is taken equal to $^{28}\sigma_{\gamma}$.

An arbitrary uncertainty of 25 % is estimated for the Yiftah data.

The uncertainty limits of the ABN data are obtained with the help of comparison of the ABN data with the Yiftah limits.

b) Fission

The fission cross section data of Yiftah are taken from Davey [27] in the energy region $1 \text{ keV} < E < 1.7 \text{ MeV}$. This evaluation of Davey is based on only one measurement with a claimed accuracy of about 10%.

Above 2 MeV the fission cross section of Pu^{242} is chosen equal to that of Pu^{240} . In this region an arbitrary uncertainty of 20% is assumed. This means that the ABN data are about equal to the lower Yiftah limits.

The estimated uncertainties are collected in table 4.7.

4.4.5. Hydrogen and oxygen

For hydrogen all nuclear data uncertainties are 1-2% or smaller.

For oxygen σ_{γ} is negligible. Cross sections for other capture processes, e.g. (n, α) , are only important at high neutron energies. The uncertainty is about $\pm 20\%$.

The inelastic scattering of oxygen occurs only above 6.5 MeV and has an uncertainty of about $\pm 30\%$.

4.4.6. The fission products of Pu^{239}

For the fission products the KFK-SNEAK set still contains the ABN data. For every fissionable material one pseudo product is available.

At the Kernforschungszentrum Karlsruhe, Hakansson [28] has determined 2 pseudo fission products for Pu^{239} . The first one collects the fission products with relative fast removal by decay or neutron capture while the second one collects the other fission products. This division into 2 classes is made in order to be able to study the effect of "fission product burn-up" being only significant for the first class. Moreover, Hakansson has calculated his group constants with the help of the

neutron energy spectrum both of a steam-cooled and a sodium-cooled fast breeder reactor instead of the Fermi spectrum for the ABN set.

Table 4.8 shows the comparison of the ABN data with the data of Hakansson combined in one pseudo fission product. Above 100 eV the data of Hakansson are considerably smaller, below 100 eV much larger than the ABN data.

The effect of fission product cross section uncertainties may be studied by changing the ABN data by the Hakansson data.

Table 4.1: Data uncertainties of Pu²³⁹

Group	Energy range	Fission		$\alpha = \sigma_c / \sigma_f$		Capture		ν		Inelastic scattering	
		+%	-%	+%	-%	+%	-%	+%	-%	+%	-%
1	6.5-10.5MeV	7	7	20	20	20	20	2	2	20	20
2	4.0-6.5	7	7	20	20	20	20	2	2	20	20
3	2.5-4.0	7	7	20	20	20	20	2	2	20	20
4	1.4-2.5	7	7	20	20	20	20	2	2	20	20
5	0.8-1.4	7	10	10	10	12	15	2	2	20	20
6	0.4-0.8	10	10	10	10	15	15	1	1	20	20
7	0.2-0.4	10	10	10	10	15	15			50	50
8	0.1-0.2	15	10	10	10	20	15			50	50
9	46.5-100keV	20	7	15	15	25	20			50	50
10	21.5-46.5	20	7	30	0	40	10			50	50
11	10.0-21.5	10	10	80	0	80	10			50	50
12	4.65-10.0	20	20	100	0	100	20				
13	2.15-4.65	20	20	100	0	100	20				
14	1.0-2.15	20	20	80	20	80	20				
15	0.465-1.0	20	20	70	0	75	20				
16	215-465eV	20	20	40	0	45	20				
17	100-215	20	20	25	0	30	20				
18	46.5-100	20	20	20	20	30	30				
19	21.5-46.5	20	20	20	20	30	30				
20	10.0-21.5	20	20	20	20	30	30				
21	4.65-10.0	15	15	20	20	25	25				
22	2.15-4.65	15	15	20	20	25	25				
23	1.0-2.15	15	15	20	20	25	25				
24	0.465-1.0	7	7	20	20	20	20				
25	0.215-0.465	7	7	10	10	15	15				
26	0.0252	2	2	3	3	3	3	1	1		

Table 4.2: Data uncertainties of U²³⁸

Group	Energy range	Capture		Fission		inelastic scattering	
		+%	-%	+%	-%	+%	-%
1	6.5MeV-10.5MeV	10	10	10	10	15	15
2	4.0 -6.5	10	10	10	10	15	15
3	2.5 -4.0	10	10	15	15	15	15
4	1.4 -2.5	10	10	7	7	20	20
5	0.8 -1.4	10	10	7	7	15	15
6	0.4 -0.8	10	10	7	7	15	15
7	0.2 -0.4	20	20	7	7	15	15
8	0.1 -0.2	20	20			15	15
9	46.5keV-100keV	20	20			15	15
10	21.5 -46.5	20	20				
11	10.0 -21.5	20	20				
12	4.65 -10	20	20				
13	2.15 -4.65	20	20				
14	1.0 -2.15	20	20				
15	0.465- 1.0	15	15				
16	215eV-465eV						
17	100 -215						
18	46.5 -100						
19	21.5 -46.5						
20	10.0 -21.5						
21	4.65 -10.0						
22	2.15 -4.65						
23	1.0 -2.15	15	15				
24	0.465-1.0	2	2				
25	0.215-0.465	2	2				
26	0.0252	1	1				

Table 4.3: Data uncertainties of Fe and Ni

Group	Energy range	Iron				Nickel			
		Capture		inelastic scattering		Capture		inelastic scattering	
		+%	-%	+%	-%	+%	-%	+%	-%
1	6.5MeV-10.5 MeV	15	15	10	10	10	10	20	20
2	4.0 -6.5	15	15	20	20	20	20	20	20
3	2.5 -4.0	15	15	30	30	20	20	20	20
4	1.4 -2.5	25	25	25	25	10	10	20	20
5	0.8 -1.4	20	20	10	10	10	10		
6	0.4 -0.8	15	15			15	15		
7	0.2 -0.4	15	15			15	15		
8	0.1 -0.2	15	15			30	30		
9	46.5keV-100keV	100	70			100	40		
10	21.5 -46.5	100	70			150	10		
11	10.0 -21.5	100	70			-	85		
12	4.65 -10.0	100	70			200	15		
13	2.15 -4.65	100	70			100	40		
14	1.0 -2.15	15	15			20	20		
15	0.465 -1.0	10	10			5	5		
16	215 eV-465eV	4	4						
17	100 -215								
18	46.5 -100								
19	21.5 -46.5								
20	10.0 -21.5								
21	4.65 -10.0								
22	2.15 -4.65								
23	1.0 -2.15								
24	0.465 -1.0								
25	0.215 -0.465								
26	0.0252	4	4			5	5		

Table 4.4: Data uncertainties of Mo and Cr

Group	Energy range	Molybdenum				Chromium			
		Capture		Inelastic scattering		Capture		Inelastic scattering	
		+%	-%	+%	-%	+%	-%	+%	-%
1	6.5MeV-10.5MeV	30	30	25	10	30	30	10	10
2	4.0 -6.5	25	25	30	0	25	25	10	10
3	2.5 -4.0	0	40	30	10	25	25	10	10
4	1.4 -2.5	0	30	25	25	25	25	20	20
5	0.8 -1.4	20	20	50	0	20	20	25	25
6	0.4 -0.8	20	20	50	0	20	20	25	25
7	0.2 -0.4	20	20	30	30	20	20		
8	0.1 -0.2	20	25			20	20		
9	46.5keV-100keV	30	30			30	30		
10	21.5 -46.5	50	0			30	30		
11	10.0 -21.5	60	0			30	30		
12	4.65 -10.0	60	0			20	20		
13	2.15 -4.65	50	0			20	20		
14	1.0 -2.15	40	0			20	20		
15	0.465 -1.0	15	15			20	20		
16	2.15eV-4.65eV					7	7		
17	100 -215								
18	46.5 -100								
19	21.5 -46.5								
20	10.0 -21.5	15	15						
21	4.65 -10.0	5	5						
22	2.15 -4.65								
23	1.0 -2.15								
24	0.465 -1.0								
25	0.215- 0.465								
26	0.0252	5	5			7	7		

Table 4.5: Data uncertainties of Nb

Group	Energy range	Capture		Inelastic scattering	
		+%	-%	+%	-%
1	6.5MeV-10.5MeV	20	20	10	10
2	4.0 -6.5	20	20	10	10
3	2.5 -4.0	20	20	10	10
4	1.4 -2.5	20	20	30	0
5	0.8 -1.4	20	20	15	15
6	0.4 -0.8	10	25	15	15
7	0.2 -0.4	10	30	15	15
8	0.1 -0.2	10	40		
9	46.5keV-100keV	10	25		
10	21.5 -46.5	10	25		
11	10.0 -21.5	10	10		
12	4.65 -10.0	15	15		
13	2.15 -4.65				
14	1.0 -2.15				
15	0.465 -1.0				
16	215eV -465eV				
17	100 -215				
18	46.5 -100				
19	21.5 -46.5	15	15		
20	10.0 -21.5	5	5		
21	4.65 -10.0				
22	2.15 -4.65				
23	1.0 -2.15				
24	0.465 -1.0				
25	0.215 -0.465				
26	0.0215	5	5		

Table 4.6: Data uncertainties of Pu^{240} and Pu^{241}

Group	Energy range	Pu^{240}				Pu^{241}			
		Capture		Fission		Capture		Fission	
		MAX (barn)	MIN (barn)	MAX (barn)	MIN (barn)	+%	-%	+%	-%
1	6.5MeV-10.5MeV	0.01	0.005	2.2	1.8	0.003b	-	50	-
2	4.0 -6.5	0.02	0.01	1.6	1.4	-	50	30	-
3	2.5 -4.0	0.04	0.02	1.6	1.4	-	50	30	-
4	1.4 -2.5	0.09	0.05	1.6	1.4	-	50	30	-
5	0.8 -1.4	0.24	0.1	1.6	1.4	-	40	10	10
6	0.4 -0.8	0.26	0.1	0.7	0.5	100	10	20	10
7	0.2 -0.4	0.34	0.12	0.17	0.13	50	10	10	10
8	0.1 -0.2	0.45	0.15	0.12	0.08	50	10	10	10
9	46.5keV-100keV	0.65	0.26	0.09	0.07	100	-	-	20
10	21.5 -46.5	0.90	0.42	0.12	0.09	80	-	-	30
11	10.0 -21.5	1.30	0.60	0.11	0.09	50	20	-	40
12	4.65 -10.0	1.80	0.85	0.12	0.08	50	20	-	30
13	2.15 -4.65	2.70	1.3	0.20	0.07	30	30	-	30
14	1.0 -2.15	4.50	3.0	0.30	0.06	15	15	-	20
15	465eV -1000eV	6.50	4.5	0.40	0.06			15	15
16	215 -465	12.0	8.0						
17	100 -215	18.0	12.0						
18	46.5 -100	49.0	33.0						
19	21.5 -46.5	44.0	30.0						
20	10.0 -21.5	28.0	19.0						
21	4.65 -10.0	0.6	0.4						
22	2.15 -4.65	6.0	4.0	0.40	0.06				
23	1.0 -2.15	14250	10600	3.0	2.0				
24	0.465-1.0	1110	780	0.4	0.1				
25	0.215-0.465	160	120	0.05	0.02	15	15	15	15
26	0.0252	295	270	0.06	0.04	20	20	3	3

Table 4.7: Data uncertainties of Pu²⁴²

Group	Energy range	Capture		Fission	
		+%	-%	+%	-%
1	6.5MeV-10.5MeV	0.01b	-	60	-
2	4.0 -6.5	30%	30%	60	10
3	2.5 -4.0	30	30	60	-
4	1.4 -2.5	30	30	50	-
5	0.8 -1.4	40	10	10	10
6	0.4 -0.8	70	10	10	10
7	0.2 -0.4	50	10	10	10
8	0.1 -0.2	40	20	10	10
9	46.5keV-100keV	50	20	10	10
10	21.5 -46.5	100	-	10	10
11	10.0 -21.5	100	-	10	10
12	4.65 -10.0	100	-	10	10
13	2.15 -4.65	70	20		
14	1.0 -2.15	15	15		
15	0.465 -1.0				
16	215eV -465eV				
17	100 -215				
18	46.5 -100				
19	21.5 -46.5				
20	10.0 -21.5				
21	4.65 -10.0				
22	2.15 -4.65				
23	1.0 -2.15				
24	0.465 -1.0				
25	0.215 -0.465	15	15		
26	0.0252	20	-		

Table 4.8: Comparison of the data by Hakansson with the ABN data for the fission products of Pu²³⁹

Group	Energy range	$\frac{\sigma_x^i \text{ HAKANSSON}}{\sigma_x^i \text{ ABN}}$			
		σ_{TOT}	σ_{γ}	σ_{el}	σ_{in}
1	6.5MeV-10.5MeV	0.77	0.37	0.84	0.69
2	4.0 -6.5	0.75	0.37	0.78	0.70
3	2.5 -4.0	0.79	0.37	0.86	0.67
4	1.4 -2.5	0.84	0.41	0.93	0.64
5	0.8 -1.4	0.87	0.70	0.95	0.50
6	0.4 -0.8	0.90	0.83	0.95	0.37
7	0.2 -0.4	0.96	0.80	0.98	0.46
8	0.1 -0.2	0.99	0.89	0.98	0.51
9	46.5keV-100keV	1.03	0.86	1.03	
10	21.5 -46.5	1.01	0.96	1.01	
11	10.0 -21.5	1.11	0.90	1.12	
12	4.65 -10.0	0.96	0.80	0.97	
13	2.15 -4.65	0.89	0.85	0.89	
14	1.0 -2.15	0.99	0.95	1.00	
15	0.465 -1.0	0.87	0.95	0.85	
16	215eV -465eV	0.94	0.93	0.94	
17	100 -215	0.72	1.03	0.58	
18	46.5 -100	0.64	0.78	0.50	
19	21.5 -46.5	1.65	1.25	2.01	
20	10.0 -21.5	1.40	1.14	1.49	
21	4.65 -10.0	1.11	0.91	1.64	
22	2.15 -4.65	1.12	1.24	1.01	
23	1.0 -2.15	0.92	0.90	1.03	
24	0.465 -1.0	2.52	3.74	1.03	
25	0.215 -0.465	1.93	2.81	1.04	
26	0.0252	15.4	19.75	1.22	

5. The Influence of the Data Uncertainties on the Reactor Parameters.

5.1. Macroscopic Cross Section Variations

In order to obtain some general information about the influence of cross section uncertainties on the reduced steam-density coefficient (R.S.D.C.) and the Doppler coefficient (D.C.) the effect of 10% increase of the macroscopic cross sections for capture and fission was considered. Only, fundamental mode calculations were made and the variations were performed in several energy regions. Table 5.1 shows the effects calculated. Presented are relative deviations determined with the formula

$$\frac{\delta X}{X} = \frac{|X_{\text{new}}| - |X_{\text{normal}}|}{|X_{\text{normal}}|} \cdot 100\% ; \quad X \equiv \begin{matrix} Y \\ \Delta k(\Delta T) \text{ (D.C.)} \\ \text{R.S.D.C} \end{matrix} \quad (6.1)$$

$\frac{\delta X}{X} = +1\%$ for the negative D.C. and R.S.D.C., means that the new calculated value of $|X|$ is 1% larger. The D.C. and R.S.D.C. are more negative.

Variation in the group	Relative deviations determined with form.(6.1)					
	Macrosc.capt.cross sect.+10%			Macrosc.fiss.cross sect.+10%		
	Y (%)	RSDC(%)	$\Delta k(\Delta T)$ (%)	Y(%)	RSDC(%)	$\Delta k(\Delta T)$ (%)
1 - 9	-2.7	-9.1	-2.9	+8.7	+14.6	+1.1
5 - 9	-2.2	-9.5	-2.5	+5.6	+19.2	+0.7
10 - 18	-5.8	+31.9	-6.3	+5.8	-27.5	+5.2
10 - 14	-3.9	+1.3	-4.2	+3.6	+4.4	+0.9
15 - 18	-2.1	+30.3	-2.3	+2.3	-32.7	+4.3
18 - 26	-0.3	+11.0	-1.8	+0.3	-10.9	+1.7
1 - 26	-8.5	+32.3	-9.4	+15.2	-22.5	+8.0

Table 5.1

From these calculations follows

- a) The influence of group cross section variations is larger for the R.S.D.C. than for the D.C.
- b) The effects due to capture and fission cross section variations are of the same order of magnitude. However, with opposite sign.
- c) The effect of variations of a cross section over the whole energy region is in rather good agreement with the sum of the effects of variations in parts of it (the effects are rather well additional over the energy region).
- d) Cross section variations at high and low energies have effects with opposite sign on the R.S.D.C. and with the same sign on the D.C.
- e) The influence on the R.S.D.C. of variations in the energy regions 50 eV to 1 keV (group 15 to 18) and 50 keV to 1 MeV (group 5 to 9) is remarkable.

In order to explain these effects qualitatively we have to examine the following aspects:

- a) The effects due to cross section variations.
- b) The origin of the R.S.D.C. and the D.C. and the way the latter are influenced by the effects due to cross section variations.

5.1.1. The effects due to cross section variations. The main effects are:

- a) Change of the quantity of fissile material required.
- b) Changes in the flux and adjoint flux spectrum.

Since in this study mainly the influences of capture and fission cross section variations are considered, here, only the effect of variations of these cross sections is examined.

If in a just critical reactor at some energy the capture cross section increases or if the fission one decreases, the reactor will become sub-critical because less neutrons are available for the multiplication process. In order to keep the reactor critical the amount of fissile material is increased (the ratio γ between fertile and fissile material decreases). For decreasing of the capture or increasing of the fission cross section the effect is just inverse (increasing of γ).

The flux $\phi(E)$ is a measure for the mean number of neutrons with energy E in the reactor.

The adjoint flux $\phi^+(E)$ may be considered to be the number of daughter neutrons of the neutron distribution due to a neutron put in the reactor with energy E .

The flux and adjoint flux spectrum are influenced by 2 effects:

- a) The initial variation of the cross sections
- b) The variation of γ (to keep the reactor critical) will influence the spectra considered because the energy dependence of the cross sections of the different fuel materials (e.g. U^{238} and Pu^{239}) is not identical.

In a first approximation the flux in group i may be considered inverse proportional to the removal cross section of this energy group and the adjoint flux proportional to the number of fission neutrons per absorption in group i :
$$\eta_i = \frac{\nu \Sigma_f^i}{\Sigma_f^i + \Sigma_\gamma^i}$$

Influence on the flux.

If the capture or fission cross section in group i increases the flux in this group will decrease relatively. The same occurs in groups with smaller energy because less neutrons come from group i . The relative decreasing of the flux in the latter groups is smaller than in group i because the hydrogen in the reactor enables "overscattering" (neutrons of group j with energy larger than group i ($j < i$) may be scattered to group $j+k$ with $j+k > i$).

Generally, variation of the cross section in group i mainly has influence on the flux in this group i and in groups with energy smaller than the energy in group i .

The dependence of the flux spectrum on the variation of Y may be shown with the help of $\frac{\partial \Sigma_{rem}}{\Sigma_{rem}} / \frac{\partial Y}{Y}$, that is the relative variation of the removal cross section with Y variation. Figure 11 shows the energy dependence of $\frac{\partial \Sigma_{rem}}{\Sigma_{rem}} / \frac{\partial Y}{Y}$ for the D-1 design. With increasing Y , Σ_{rem} decreases more for low energies than for the high ones. This means that for increasing Y the neutron flux spectrum will become softer.

Influence on the adjoint flux.

If the capture cross section in group i increases the adjoint flux in this group will decrease (less daughter neutrons are produced by neutrons put in the reactor with energies of group i). Increasing of the fission cross section has the opposite effect: more daughter neutrons and larger adjoint flux in group i . These effects described are also noticeable in the energy groups with larger energy than group i because neutrons put in the reactor with energies larger than group i result in a neutron spectrum with neutrons in group i . In the energy groups with smaller energies the adjoint flux is hardly influenced.

Analyses of the dependence of η on the variation of Y did not show significant energy dependence of $\partial \eta / \partial Y$. So, in a first approximation we may assume that the adjoint flux spectrum is not influenced significantly by the variations of Y .

5.1.2. The origin of the D.C. and R.S.D.C. and the way the latter are influenced by the effects due to cross section variations.

5.1.2.1. The Doppler Coefficient D.C.

The Doppler effect is the reactivity effect caused by the temperature dependent variations of the cross sections in the resonance region. The D.C. is dependent on the ratio between the capture and fission cross section variations and on the relative magnitude of the flux and adjoint flux in the energy region where the cross section temperature dependence

is significant. Since U^{238} has negative Doppler effect and Pu^{239} has none or a small positive one the total effect is dependent on the ratio between these materials (the ratio γ).

In table 5.1 the variation of $\Delta k(T=900-2100)$ is identical with the variation of the D.C. We may observe that the D.C. variations have the same sign as the γ variations in all calculated cases. This means that increasing of γ results in a more negative D.C. Dependent on other influences due to the cross section variations, the change of the D.C. is larger or smaller than the change in γ .

For variations in the energy region above 50 keV (group 1 to 9) the most significant second effect is the variation of the flux spectrum. Increasing of the capture and fission cross sections in this energy region causes a relative decreasing of the flux in the resonance region, resulting in a less negative D.C. Both for the capture and fission cross section variations this effect may be observed.

For variations in the energy region below 50 eV (group 19 to 26) the most significant second effect is the variation of the adjoint flux spectrum in the resonance region. Increasing of the capture cross section below 50 eV results in decreasing of the adjoint flux above 50 eV (also in the important resonance region) and in a less negative D.C. Increasing of the fission cross section results in increasing of the adjoint flux in the resonance region and in a more negative D.C. Both effects may be observed.

In the energy region $50\text{eV} \leq E < 50\text{keV}$ both effects due to flux and adjoint flux variations occur. A further significant effect in this region is the influence of the cross section variation itself. In the calculation method applied the temperature dependence of the self-shielding factors is independent of the group cross section variations. This means that in the case of increasing of the capture cross section in the resonance region the D.C. will be more negative due to the larger difference between the cross sections at 900°K and 2100°K . The same holds for variations of the fission cross sections in this region. However, now the D.C. will be less negative.

This effect may be observed in the case of variations in group 15 to 18.

5.1.2.2. Reduced steam-density coefficient R.S.D.C.

The R.S.D.C. is a measure for the reactivity effect due to variation of the steam-density. As for steam the absorption may be neglected practically the R.S.D.C. is mainly caused by the variation in the spectral distribution of the flux and adjoint flux due to the moderation changed. It may be noticed that the R.S.D.C. would be zero in the case of a constant adjoint flux over the whole energy region. In this case variation of the flux energy spectrum does not result in a reactivity effect.

Increasing of the steam-density has the consequence that the neutrons are moderated stronger. In the case where the adjoint flux decreases with decreasing energy the reactivity effect is negative (less neutrons are produced) while in the case of increasing adjoint flux with decreasing energy the reactivity effect will be positive. Moreover, the reactivity effect is proportional to the flux.

A good measure for the adjoint flux spectrum is the energy dependence of $\eta = \frac{\nu \Sigma_f}{\Sigma_f + \Sigma_\gamma}$. In figure 12 η and ϕ^+ are plotted as a function of the energy (for the D-1 design). For energies $10\text{keV} < E < 10\text{MeV}$ η is decreasing with decreasing energy. This means that in this region for increased steam-density a negative reactivity effect may be expected. In the energy region $100\text{eV} < E < 10\text{keV}$ η increases with decreasing energy. The reactivity effect is expected to be inverse to the effect for energies $E > 10\text{keV}$. For energies below 100eV η is fluctuating. However, in this region the flux has decreased considerably and the expected reactivity effect will be small. These quantitative considerations are in good agreement with results from perturbation calculations (see figure 7).

The influence of cross section variations on the R.S.D.C. is dependent on the way its negative and positive components are changing.

These components may be changed mainly by:

a) Hardening of the neutron spectrum:

The negative component gets more important and the R.S.D.C. will become more negative.

- b) Variation of the course of the adjoint flux at energies above 10 keV:

Flattening results in a smaller negative component and the R.S.D.C. will be less negative.

- c) Variation of the course of the adjoint flux at energies below 10 keV:

In this case flattening results in a smaller positive component and the R.S.D.C. will become less positive (or more negative).

- d) Variation of the relative difference of the adjoint flux at energies above and below 10 keV:

If this difference decreases the R.S.D.C. will become less negative (or more positive).

With the help of these considerations the effect of cross section variations on the R.S.D.C. may be explained qualitatively. Significant for the effects are the variations of the adjoint flux.

For one case the effect will be analysed in more detail.

10% increase of Σ_{γ} in the groups 5 to 9

The following effects occur:

- a) γ decreases. The neutron flux spectrum becomes harder. The R.S.D.C. becomes more negative.
- b) Due to the Σ_{γ} variations in the group 5 to 9 the neutron flux spectrum becomes softer. The R.S.D.C. will become less negative.
- c) Due to the Σ_{γ} variations the course of the adjoint flux in the energy range above 10 keV will become steeper. The R.S.D.C. becomes more negative.
- d) Due to the Σ_{γ} variations the differences between the adjoint flux below and above 10 keV decrease. This effect results in a less negative R.S.D.C.

The points a) through d) show influences with opposite sign on the R.S.D.C. Namely, a negative variation of the R.S.D.C. due to the points a) and c) and a positive variation due to the points b) and d).

The calculations in table 5.1 give a positive change of the R.S.D.C. Further analyses of the influence of the points a) through d) show that the main effect comes from the point d): the variation of the difference between the adjoint flux above and below 10 keV.

Some general remarks with respect to the influence of the cross section variations on the R.S.D.C.:

- a) Variations of the capture and fission cross sections generally have opposite influence because the effects of these variations on the adjoint flux are opposite.
- b) Variations in the groups 10 to 14 only have small not well defined influence for 2 reasons:
 - The relative variations in the adjoint flux are not very large. Moreover, both the positive and the negative components are influenced simultaneously. These effects counterbalance each other partly.
 - More extensive investigations of this energy region for material dependent cross section variations showed that changes in the groups 10 to 12 have opposite effect with respect to variations in the groups 13 and 14.
- c) Variations in the groups 5 to 9 have large influence since the effect on the negative component of the R.S.D.C. due to the changing difference between the adjoint flux above and below 10 keV is relatively large.
- d) Variations in the groups 15 to 18 have large influence because the effect on the positive component of the R.S.D.C. due to the variation of the course of the adjoint flux below 10 keV is relatively large.

5.1.3. The maximum variation of the R.S.D.C. obtained by 10% changes of the macroscopic capture and fission cross sections.

Finally, some group constants for capture and fission were changed by 10% in a way that

- a) the variation of γ was small
- b) the R.S.D.C. became most positive and most negative.

Table 5.2 shows the variations performed. The calculated parameters with the variations of table 5.2. shows table 5.3.

Group		5-9	10-14	15-18
Most positive R.S.D.C.	Σ_{γ}^i	+10%	-	-10%
	Σ_f^i	-10%	+10%	+10%
Most negative R.S.D.C.	Σ_{γ}^i	-10%	-	+10%
	Σ_f^i	+10%	-10%	-10%

Table 5.2

	$\frac{\delta \gamma}{\gamma}$ (%)	$\frac{\delta \text{RSDC}}{\text{RSDC}}$ (%)	$\frac{\delta k(\Delta T)}{k(\Delta T)}$ (%)
Most positive R.S.D.C.	+0.44	-91.6	+3.7
Most negative R.S.D.C.	-0.37	+88.0	-4.7

Table 5.3

The influence appeared to be rather well additional.

Already from these calculations follows that the R.S.D.C. is very sensitive to cross section uncertainties and may vary over a wide range.

5.2. The influence of the data uncertainties of the reactor materials.

As described in chapter 2 the parameters considered are D.C., R.S.D.C., Δk_L , γ and C.R.

The investigations of the influence of macroscopic cross section variations (chapter 5.1.) showed that the R.S.D.C. is very sensitive to cross section variations in the energy range where the Doppler effect is dominant. Therefore, the temperature dependence of the R.S.D.C. and the Δk_L is investigated too. The values calculated at 900°K and 2100°K with the KFK-SNEAK set are given in table 5.4.

T °K	R.S.D.C.	Δk_L
900	$-2.14 \cdot 10^{-2}$	$3.6384 \cdot 10^{-2}$
2100	$-2.58 \cdot 10^{-2}$	$4.3842 \cdot 10^{-2}$

Table 5.4

Evidently, the differences are rather large. The reason that the R.S.D.C. becomes more negative with increasing temperature may be explained by the influence of a temperature change on the adjoint flux spectrum. Increasing of the temperature causes increasing of the effective cross sections for capture and fission in the resonance energy range. Since the D.C. is negative the increasing of the effective capture cross section is dominant. This means that in this energy region the adjoint flux decreases, resulting in a smaller positive component of the R.S.D.C. (see chapter 5.1.2.2.). At the time where the investigations of the influence of the data uncertainties were started the preparation of the KFK-SNEAK set was not yet completed entirely. The self-shielding factors of Pu²³⁹ were still taken from the ABN set. That is why most influences of group constant variations are calculated with respect to the KFK-SNEAK set with old f-factors for Pu²³⁹.

In table 5.5 the parameters calculated with the old and new f-factors for Pu²³⁹ are given.

KFK-SNEAK set with	Y	C.R.	$\Delta k_L / \beta$ *)		R.S.D.C. · 10 ²		$A_D \cdot 10^2$ **)
			T = 900°K	T = 2100°K	T = 900°K	T = 2100°K	
Old f-factors for Pu ²³⁹	7.40758	0.9952	+12.96	+14.55	-2.52	-2.74	-1.0662
New f-factors for Pu ²³⁹	7.39310	0.9857	+11.30	+13.61	-2.14	-2.58	-1.3857

Table 5.5

*) $\beta \approx 0.00322$

**) A_D is the Doppler constant, assuming the temperature dependence $D.C. = \frac{A_D}{T}$

For the important parameters the differences are remarkable.

Since not all calculations could be done with the help of the final KFK-SNEAK set the results will be presented as absolute parameter variations. Only for the ratio Y the relative deviation $\frac{\partial Y}{Y}$ is given.

The uncertainties of the most important cross-sections of the reactor materials are collected in the tables 4.1 to 4.8.

In the cases the upper and lower limits have the same deviation from the data of the KFK -SNEAK set usually only the effect of the upper limit is calculated.

Some comparison calculations showed that the absolute value of the effects due to equal positive and negative variations of the group constants are not the same exactly. However, the differences observed are relatively small.

For the inelastic cross section only the total value was varied. The transfer probabilities were kept constant. This means that with

$$\Sigma_{IN}^i = \sum_j \Sigma_{i \rightarrow j}$$

that

Σ_{IN}^i and $\Sigma_{i \rightarrow j}$ were varied in the same way.

The influence of the data uncertainties of Pu²³⁹ and U²³⁸ is investigated most extensively because the latter have the largest atom density of the materials with considerable data uncertainties.

The variations of the parameters D.C. and R.S.D.C. due to the data uncertainties show the same behaviour as the effects due to the macroscopic cross section variations described in chapter 5.1.

5.2.1. Pu²³⁹

The variations caused by the data uncertainties of Pu²³⁹ are collected in table 5.8. These deviations may be compared with the parameters of table 5.5.

The main influence on the parameters considered is due to the fission and capture cross section uncertainties in the energy range 50 eV to 10 keV. It also may be observed that the measurements of Schomberg et al. [20] influence the C.R. and the R.S.D.C. very unfavourably (see also chapter 6). The influence of the inelastic scattering uncertainties is small. Since the R.S.D.C. is important for the stability and the dynamic behaviour of the reactor and also very sensitive to cross section variations the maximal expected influence on this parameter due to the data uncertainties of Pu²³⁹ is calculated (table 5.6).

Variations of σ_y and σ_f of Pu ²³⁹ in a way that	Y	C.R.	Δk_L %		RSDC $\cdot 10^2$		$A_D \cdot 10^2$
			T=900°K	T=2100°K	T=900°K	T=2100°K	
RSDC most positive	7.33667	0.9707	- 3.65	- 1.00	+1.365	+0.86	-1.6697
RSDC most negative	7.33477	0.8931	+31.57	+33.39	-6.455	-6.82	-1.0704

Table 5.6

5.2.2. U²³⁸

Table 5.9 gives the variations due to the data uncertainties of U²³⁸. The largest influences come from the capture cross section uncertainties in the groups 5 to 9 and 15 to 18. It may be observed that for the variation in the groups 15 to 18 the influence on the D.C. by the variation of the ratio γ is overcompensated by the increasing of the capture cross section in the resonance region of U²³⁸ (compare with chapter 5.1.2.1.).

The influence of the inelastic cross-section uncertainties of U²³⁸ is small. For the other reactor materials the influence of the inelastic cross section uncertainties will not be calculated.

The most negative R.S.D.C. caused by the data uncertainties of U²³⁸ is given in table 5.7.

Variation	γ	C.R.	Δk_L		RSDC · 10 ²		$A_D \cdot 10^2$
			T=900°K	T=2100°K	T=900°K	T=2100°K	
For U ²³⁸ Min Gr. 1 to 11 Max Gr. 12 to 26	σ_y 7.44384	0.9857	+18.14	+20.67	-3.36	-3.76	-1.5053

Table 5.7

5.2.3 The higher Pu isotopes

For the higher Pu isotopes less calculations are performed.

For the Pu²⁴⁰ the parameters are calculated for 3 cases.

- a) With the data recommended by Yiftah [18]
- b) With the minimum expected capture cross sections
- c) With the data recommended by Pitterle [19] (MOD-ENDF/B)

With the data of Yiftah the D.C. and R.S.D.C. become slightly more unfavourable. Due to the smaller capture cross sections the data of Pitterle give parameters considerably more favourable.

For Pu²⁴¹ the influences on the parameters are still considerably smaller. In some energy regions the influence of the largest data uncertainties is calculated. The same was done for Pu²⁴².

The results are collected in table 5.10.

5.2.4. The structural materials, the fission products and oxigen.

The influence of the data uncertainties of Ni is examined in detail. For the other materials only one calculation is made. The influences observed are small. The results are collected in table 5.11.

Table 5.8

Variations	$\Delta y/y$ (%) ^{*)}	$\delta C.R. \cdot 10^2$ *)	$\delta \Delta k_L$ % *)		$\delta RSDC \cdot 10^2$ *)		$\delta A_D \cdot 10^2$ *)
			T=900°K	T=2100°K	T=900°K	T=2100°K	
σ_Y MAX ALL GROUPS	-7.36	-6.98	+6.18	+6.00	-1.17	-1.15	+0.1846
σ_Y MAX GR 1-4	-0.01	-0.01	0.0	+0.09	0.0	-0.01	0.0
σ_Y MAX GR 5-9	-0.38	-0.97	-0.40	-0.25	+0.045	+0.05	+0.0049
σ_Y MAX GR 10-14	-4.12	-10.39	+2.07	+2.01	-0.155	-0.16	+0.1019
σ_Y MAX GR 10-11	-1.05	-2.96	-0.32	-0.32	+0.075	+0.07	+0.0185
σ_Y MAX GR 12-14	-3.11	-7.75	+2.34	+2.29	-0.225	-0.23	+0.0840
σ_Y MAX GR 15-18	-2.65	-5.34	+3.93	+3.83	-0.87	-0.86	+0.0692
σ_Y MAX GR 19-26	-0.28	-0.63	+0.47	+0.45	-0.205	-0.19	+0.0099
σ_Y MIN GR 12-18	+2.14	+4.86	-2.67	-2.61	+0.575	+0.59	-0.0517
σ_Y MIN GR 5-11	+0.49	+1.33	+0.27	+0.28	-0.055	-0.05	-0.0071
σ_F MAX ALL GROUPS	+5.08	+4.27	-3.56	-3.37	+0.91	+0.88	-0.1621
σ_F MAX GR 1-4	+0.77	+0.23	-0.13	-0.13	+0.02	+0.02	-0.0018
σ_F MAX GR 5-9	+6.89	+1.44	+3.85	+3.87	-0.735	-0.73	-0.0082
σ_F MAX GR 10-14	+5.91	+1.36	-0.56	-0.57	-0.14	-0.13	-0.0161
σ_F MAX GR 10-12	+3.35	+0.72	+1.29	+1.29	-0.285	-0.28	-0.0043
σ_F MAX GR 13-14	+2.56	+0.50	-1.89	-1.90	+0.145	+0.15	-0.0120
σ_F MAX GR 15-18	+4.15	+1.32	-6.07	-5.95	+1.43	+0.24	-0.0779
σ_F MAX GR 19-26	+0.51	+0.05	-0.86	-0.81	+0.375	+0.36	-0.0232
σ_F MIN GR 5-12	-6.00	-1.37	-2.90	-2.92	+0.575	+0.58	+0.0092
σ_{IN} MAX GR 1-11	-0.16	-0.12	-0.05	-0.05	+0.01	+0.01	-0.0011

*) For the values of the parameters see table 6.5
Influence of cross-section uncertainties of Pu²³⁹

Table 5.9

Variation	$\partial y/y$ (%)**)	$\partial C.R. \cdot 10^2$ **)	$\delta A_{K_L} \text{ } \text{\$ } \text{**})$		$\delta RSDC \cdot 10^2$ **)		$\delta A_D \cdot 10^2$ **)
			T=900°K	T=2100°K	T=900°K	T=2100°K	
σ_f MAX GR 1- 7	+1.73	+1.47	-0.42	-0.31	+0.06	+0.05	-0.0041
σ_Y MAX ALL GROUPS	-8.32	+7.16	+1.71	+1.75	-0.29	-0.34	+0.0285
σ_Y MAX GR 1- 4	-0.10	+0.03	+0.01	+0.01	0.0	0.0	+0.0009
σ_Y MAX GR 1- 9	-2.68	+1.44	-1.58	-1.63	+0.285	+0.28	+0.0383
σ_Y MAX GR 5- 9	-2.60	+1.82	-1.59	-1.63	+0.29	+0.28	+0.0375
σ_Y MAX GR 10-14	-4.72	+1.63	+1.30	+1.32	-0.055	-0.07	+0.0260
σ_Y MAX GR 15-18	-1.27	+1.14	+1.87	+1.99	-0.415	-0.46	-0.0762
σ_Y MAX GR 19-26	-0.13	+0.18	+0.29	+0.28	-0.125	-0.23	+0.0032
σ_{IN} MAX GR 1- 4	-1.48	-0.86	+0.16	+0.16	-0.015	-0.02	-0.0021
σ_{IN} MAX GR 1- 9	-1.79	-0.94	-0.22	-0.22	+0.05	+0.05	-0.0069

**) For the values of the parameters see table 6.5
Influence of cross-section uncertainties of U^{238}

Table 5.10

Material	Variation	$\partial y/y$ (%) ^{*)}	$\partial C.R. \cdot 10^2$ ^{*)}	$\delta A_{k, l}$ %		$\delta RSDC \cdot 10^2$ ^{*)}		$\delta A_D \cdot 10^2$ ^{*)}
				T=900°K	T=2100°K	T=900°K	T=2100°K	
Pu ²⁴⁰	DATA BY YIFTAH	+1.18	+0.99	+0.11	+0.12	-0.035	-0.04	-0.0093
	σ_Y MIN ALL GROUPS	+3.15	-2.56	-1.19	-1.13	+0.29	+0.29	-0.0663
	MOD.ENDF/B by Pitterle	+5.30	-0.77	-1.32	-1.23	+0.295	+0.30	-0.0856
Pu ²⁴¹	σ_Y GR 1-9 MAX	-1.45	-0.42	+0.83	+0.78	-0.15	-0.13	+0.0316
	GR 10-26 MIN							
	σ_f GR 1-5 MAX	+0.10	0.0	-0.02	-0.02	-0.01	0.0	-0.0001
	σ_f GR 6-10 MIN	-0.42	-0.10	-0.33	-0.33	+0.055	+0.06	+0.0006
	σ_f GR 11-14 MIN	-0.74	-0.20	+0.14	+0.14	-0.15	-0.19	+0.0034
	σ_f GR 15-18 MAX	+0.20	+0.07	-0.30	-0.28	+0.065	+0.07	-0.0457
	σ_Y GR 1-26 MAX	-0.38	-0.93	+0.43	+0.37	-0.175	-0.14	+0.0237
	σ_Y GR 6-11 MAX	-0.08	-0.21	-0.05	-0.05	+0.01	+0.01	+0.0010
σ_Y GR 12-26 MAX	-0.30	-0.36	+0.48	+0.45	-0.18	-0.16	+0.0238	
Pu ²⁴¹	σ_Y GR 1-11 MAX	-0.04	-0.04	-0.02	-0.02	+0.005	0.0	+0.0007
	σ_Y GR 12-26 MAX	-0.04	-0.03	+0.04	+0.04	-0.005	0.0	+0.0016
	σ_f GR 1-6 MAX	+0.06	+0.05	-0.01	-0.01	0.0	+0.01	-0.0001

*) For the values of the parameters see table 6.5
Influence of the cross-section uncertainties of the higher Pu isotopes.

Table 5.11

Material	Variation	$\partial y/y$ (%) ^{*)}	$\partial C.R. \cdot 10^2$ *)	$\delta \Delta K_L$ \$ *)		$\delta RSDC \cdot 10^2$ *)		$\delta A_D \cdot 10^2$ *)
				T=900°K	T=2100°K	T=900°K	T=2100°K	
Ni	σ_Y MAX GR 1-18	-1.68	-1.52	+0.04	+0.02	+0.02	+0.02	+0.0279
	σ_Y MAX GR 1-4	-0.56	-0.46	+0.06	+0.05	-0.015	0.0	+0.0046
	σ_Y MAX GR 5-9	-0.35	-0.34	-0.25	-0.26	+0.045	+0.05	+0.0047
	σ_Y MAX GR 10-14	-0.77	-0.72	+0.21	+0.20	-0.05	-0.01	+0.0175
	σ_Y MAX GR 15-18	-0.02	-0.01	+0.02	+0.02	+0.01	0.0	+0.0011
Nb	σ_Y MAX GR 1-17	-0.44	-0.36	+0.28	+0.27	+0.04	+0.04	+0.0148
Cr	σ_Y MAX GR 1-18	-0.15	-0.14	+0.02	+0.02	0.0	0.0	+0.0036
Fe	σ_Y MAX GR 1-18	-0.10	-0.09	-0.02	-0.02	+0.005	+0.01	+0.0019
Mo	σ_Y MIN GR 1-10 MAX GR 11-20	-0.69	-0.56	+0.74	+0.70	-0.12	-0.11	+0.0292
F.P.	DATA OF HAKANSSON	+0.75	+0.55	-0.17	-0.16	0.0	0.0	-0.0144
O	σ_Y MAX GR 1-3 σ_{IN} MAX GR 1	-0.16	-0.16	+0.02	+0.02	-0.01	0.0	+0.0008

*)

For the values of the parameters see table 6.5

Influence of the cross-section uncertainties of the structural materials, the fission products (F.P.) and oxygen.

6. The Influence of the Data Uncertainties on the Safety, Stability and Dynamic Behaviour of the D-1 Design

At the Kernforschungszentrum Karlsruhe several extensive studies on the safety, stability and dynamic behaviour of the D-1 design are performed [29,30,31,32,33,34,35,36,7].

Here the influence of the data uncertainties on the following subjects will be considered:

- a) Safety
- b) Stability of the reactor core
- c) Stability of the reactor plant
- d) The dynamic behaviour of the core after a large disturbance in the cooling circuit.

6.1. The uncertainty of the most important parameters

6.1.1. The uncertainty of the R.S.D.C. and Δk_L

The investigations have shown that the influence of the data uncertainties on these parameters is very large. The outside values caused by the uncertainties of Pu^{239} and U^{238} are given in table 6.1. The influence of the other materials is relatively small.

Variation of $Pu^{239} + U^{238}$ data in a way that	Y	C.R.	Δk_L ‰		RSDC $\cdot 10^2$		$A_D \cdot 10^2$
			T=900°K	T=2100°K	T=900°K	T=2100°K	
RSDC most positive	7.62523	0.9529	-11.90	-9.37	+3.555	+2.65	-1.5192
RSDC most negative	7.38024	0.8954	+38.70	+40.44	-7.80	-8.11	-1.0509

Table 6.1

The difference between fundamental mode and more detailed calculations is small. E.g. the difference between the R.S.D.C. determined at 900°K with a fundamental mode calculation and with a 1-dimensional multi-group calculation taking into account the axial variation of the steam-density is considerably smaller than the difference between the R.S.D.C. calculated at 900°K and 2100°K with fundamental mode calculations.

6.1.2. The uncertainties of the D.C.

The D.C. is not very sensitive to the nuclear data uncertainties. The influences observed are smaller than 25%.

However, the uncertainty of the D.C. caused by the discrepancy between the different calculation methods is important too.

Comparison calculations showed that the method of Froelich systematically gives a D.C. about 15% more negative than the method of successive k-calculation.

6.2. The influence on the safety

Some preliminary calculations for the D-1 design showed a nearly inverse proportionality between the absolute value of the Dopplerconstant $A_D = T \frac{dk}{dT}$ and the energy released in a reactor excursion [37].

As may be observed in fig. 17 the value of the R.S.D.C. (and Δk_L) strongly influences the reactivity ramp after a large disturbance in the cooling circuit. Therefore, particularly the uncertainty of the R.S.D.C. and Δk_L have large influence on the safety of the D-1 design.

6.3. The stability of the core

The core stability of a steam cooled fast power reactor is examined extensively by Frisch [29]. A significant criterion for the core stability is the power coefficient of the core. A computer code was developed to calculate the relative power coefficient A taking into account most non-linearities.

$$A = \frac{\delta k_f}{\Delta P/P} \frac{1}{\beta} \quad \text{\%} \quad (6.1)$$

δk_f feedback reactivity

$\frac{\Delta P}{P}$ relative power variation

β fraction of delayed neutrons.

Note: A relative power coefficient $A = -1 \%$ means that for a relative power variation $\frac{\Delta P}{P} = 0.01$ a negative feedback reactivity $\delta k_f = -0.01 \%$ will arise.

In table 6.2 the relative power coefficient A is calculated for some cases. The relative power variation for the calculation was $\frac{\Delta P}{P} = 0.01$.

Description	A %
KFK-SNEAK SET	-1.253
σ_f of Pu ²³⁹ MAX in GR. 5-9	-0.770
σ_f of Pu ²³⁹ MAX in GR. 15-18	-2.385
σ_γ of Pu ²³⁹ MAX in GR. 5-9	-1.287
σ_γ of Pu ²³⁹ MAX in GR. 15-18	-0.516
σ_γ of U ²³⁸ MAX in GR. 5-9	-1.401
σ_γ of U ²³⁸ MAX in GR. 15-18	-1.083
DATA of Pu ²³⁹ FAVOURABLE	-4.307
DATA of Pu ²³⁹ UNFAVOURABLE	+1.858
DATA of U ²³⁸ FAVOURABLE	-2.086
DATA of U ²³⁸ UNFAVOURABLE	-0.447
FOR Pu ²⁴⁰ MOD. ENDF/B DATA	-1.638
FOR Pu ²³⁹ DATA OF SCHOMBERG	-0.163

Table 6.2

A strongly depends on the Doppler coefficient and on the steam density coefficient. Therefore, Frisch [29] has determined the boundary for $A=0$ dependent on the R.S.D.C. and the D.C. This boundary for $A=0$ slightly depends on the relative power variation $\frac{\Delta P}{P}$ and on the power level P .

The regions for inherent stability of the D-1 core as determined by Frisch are given in figure 13. In this R.S.D.C.-D.C. plane some significant results of the present study are plotted. It is assumed that the other reactivity effects are not influenced by the data uncertainties. In figure 13 also are plotted the uncertainties of the D.C. caused by the discrepancy between the calculation methods and the variation of the R.S.D.C. caused by a temperature change of $T=900^{\circ}\text{K}$ to $T=2100^{\circ}\text{K}$.

With the nuclear data of the KFK-SNEAK set the reactor is inherent stable. The new α -measurements for Pu^{239} by Schomberg et al. [20] are very unfavourable for the stability.

The most recent evaluation of the data for Pu^{240} (the mod. ENDF/B data by Pitterle [19]) has a favourable influence on the stability.

Due to the possible data uncertainties of Pu^{239} and U^{238} the R.S.D.C. may become so far negative that the reactor is unstable. The R.S.D.C. also may become positive. In this case the reactor plant will be unstable without a control system. However, it may be expected that the R.S.D.C. will not become so much positive that oscillatory instability of the core will occur. (See [30])

6.4. The stability of the plant

In [29] it is shown that it is impossible to obtain a stable reactor plant with an unstable core and that the R.S.D.C. has to be negative. For a reactor plant with a stable core the stability strongly depends on the delay times in the cooling circuit [35]. In [33] it is pointed out that power oscillations are prevented if:

$$K_k \cdot \alpha_p \cdot \frac{dp}{dT} \cdot \frac{V^*P}{C} \cdot T_u < A_{\text{crit}} \quad (6.2)$$

with

$K_k = \frac{\Delta P/P}{\Delta k}$: reactivity gain. After a reactivity disturbance Δk , the power level increases from P to $P+\Delta P$

α_ρ steam-density coefficient

ρ steam-density

p steam-pressure

y ratio of the quantity of superheated steam flowing to the evaporators to the total quantity of steam flowing through the core.

C energy storage capacity of the coolant system

T_u delay time

A_{crit} depends on the composition of the delay time T_u and has a minimum of $\frac{\pi}{2}$ under the assumption of a pure dead time. In the case of 2 delay times of equal length A_{crit} becomes 4. In [35] it is shown that in the case of several time constants of the same order of magnitude (as in the D-1 design) A_{crit} lies between:

$$\frac{\pi}{2} < A_{crit} < 4 \quad (6.3)$$

The left hand side component of formula (6.2)

$$B = K_k \cdot \alpha_\rho \cdot \frac{dp}{dp} \cdot \frac{y \cdot P}{C} \cdot T_u \quad (6.4)$$

may be calculated with the help of a digital computer code.

For 3 cases of an inherent stable core the value B of formula (6.4) is calculated (table 6.3). The following realistic quantities for the D-1 design are used:

$$y = 0.64$$

$$P = 2500 \text{ MWth}$$

$$C = 500 \frac{\text{MWh}}{\text{ata}}$$

$$T_u = 4.2 \text{ sec} \quad (T_u \text{ is composed by a dead time } 0.7 \text{ sec, a delay time of } 1.5 \text{ sec for the heating of the structure material and the pipes and a delay time of } 2 \text{ sec for the heat exchange between the fuel and the coolant}).$$

Case	Description	B (form.6.4)	Comment
1	KFK-SNEAK SET	0.629	$< A_{crit}$
2	MOD. ENDF/B DATA for Pu ²⁴⁰	0.640	$< A_{crit}$
3	σ_{γ} of Pu ²³⁹ DATA by Schomberg	4.640	$> A_{crit}$

Table 6.3

In the cases 1 and 2 the behaviour of the plant will be satisfactory. However, in the case 3 after a reactivity disturbancy power oscillations will arise.

6.5. The dynamic behaviour of the core

The influence of the uncertainties on the dynamic behaviour of the reactor core after the most severe credible failure of the D-1 design (the rupture of a sigle main coolant pipe in the region of the reactor inlet [307]) was examined with the help of a digital computer program developed by Hornyik [367]. The transients were calculated for the 3 cases of table 6.4.

Case	Description	$A_D \cdot 10^2$	RSDC $\cdot 10^2$
a	KFK-SNEAK SET	-1.386	-2.14
b	FAVOURABLE DATA Pu ²³⁹	-1.55	+1.365
c	σ_{γ} DATA SCHOMBERG	-1.30	-3.55

Table 6.4

In figure 14 the maximal fuel and can temperatures of the hot channel, the thermal power and the feedback reactivity as a function of the time after the pipe rupture are plotted.

The figures 15 to 17 show the differences for these quantities for the cases a, b and c of table 6.4.

For the positive R.S.D.C. no danger for the core occurs immediately after the failure. The can temperature increases slightly due to the fact that the cooling becomes worse.

For the data by Schömberg the fuel melting already occurs after 0.33 sec instead of 0.75 sec for the parameters calculated with the KFK-SNEAK set. For the case where the R.S.D.C. is influenced most unfavourably by the data uncertainties of Pu²³⁹ it was examined if a scram could save the core from damage if a main pipe rupture near the reactor inlet occurs. It is assumed that the scram begins 0.1 sec after that where the power level has increased 25%. In figure 18 the reactivity effects are plotted and in figure 19 the can and fuel temperatures in the hot channel. In this case the core will be destroyed after the failure described.

7. Conclusions

The investigations of this study may be summarized with the following conclusions:

- 1) The Doppler coefficient D.C. is not very sensitive to the nuclear data uncertainties of the reactor materials. (The variations of the D.C. are smaller than 25%.) An important part of the variations of the D.C. due to group constant variations comes from the change of the ratio γ (fertile to fissile material).
- 2) The reduced steam-density coefficient R.S.D.C. and Δk_L are very sensitive to the uncertainties of the capture and fission cross-sections and may vary over a wide range. The dependence of the R.S.D.C. on the cross-section variations may be explained qualitatively mainly with the influence of these cross-section variations on the adjoint flux (chapter 5.1.2.2.).
- 3) The uncertainties of the capture and fission cross-sections of Pu²³⁹ and U²³⁸ have most influence on the parameters considered. The influence of the data uncertainties of the higher Pu isotopes is considerable. The other materials only have small effects.

- 4) Since the R.S.D.C. may vary over a wide range the stability, safety and dynamic behaviour of the D-1 design is influenced strongly by the nuclear data uncertainties.

With the data of the KFK-SNEAK set the D-1 design is inherent stable. The most recent data for Pu²⁴⁰ by Pitterle [19] have a favourable effect on the D.C. and the R.S.D.C.

On the other hand these parameters D.C. and R.S.D.C. are influenced unfavourably by the recent measurements by Schomberg et al. [20] for

$$\alpha = \frac{\sigma_{\gamma}}{\sigma_f} \text{ of Pu}^{239}.$$

- 5) The uncertainty of the D.C. and the R.S.D.C. of the D-1 design may be reduced significantly if:
- a) The discrepancy between the different calculation methods for the D.C. is removed.
 - b) The uncertainties of the capture and fission cross-sections of Pu²³⁹ and U²³⁸ would be reduced, particularly in the energy ranges 50 eV to 1 keV and 10 keV to 1 MeV.
- 6) Very probably the investigation of the dynamic behaviour will be improved if the dependence of the steam-density coefficient on the fuel temperature will be considered. Particularly, in the cases the fuel temperature varies considerably.

ACKNOWLEDGEMENTS

I wish to express my gratitude to Professor Dr. M. Bogaardt and to Professor Dr. K. Wirtz for the opportunity to do the final part of my study in the Institut für Neutronenphysik und Reaktortechnik at the Kernforschungszentrum Karlsruhe.

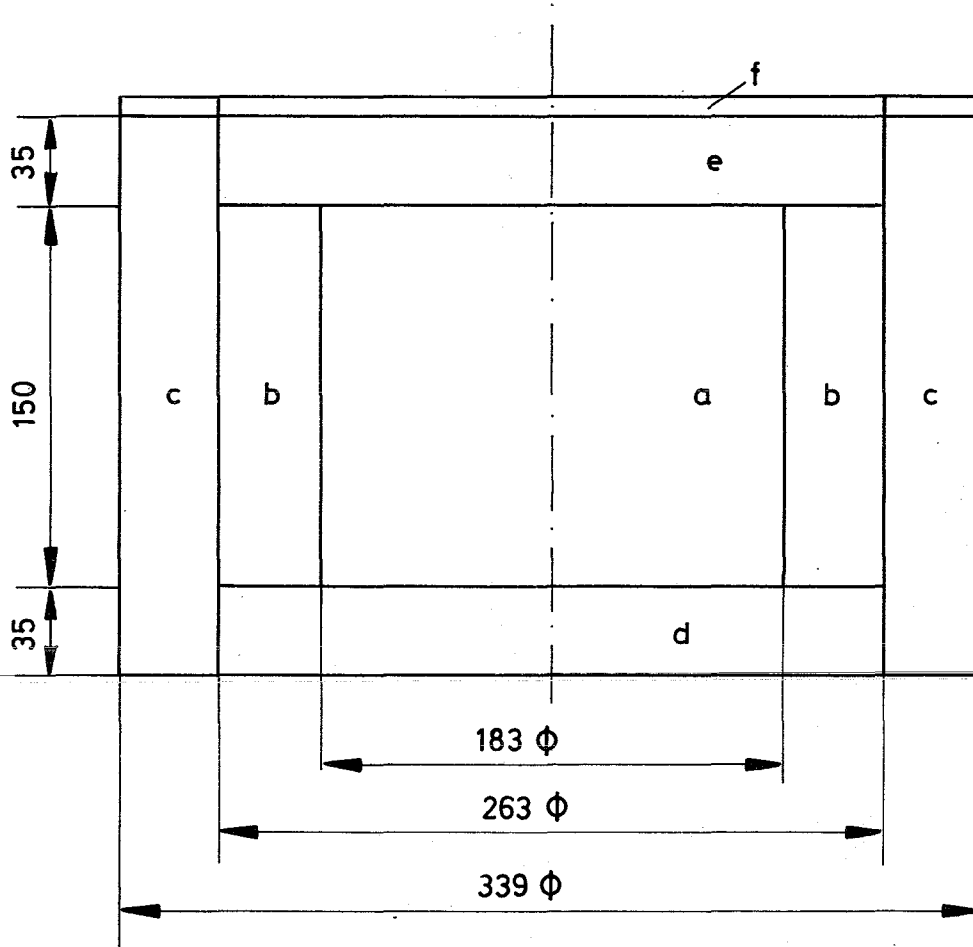
All members of the I.N.R. I want to thank for their patience and willingness to help me with my problems. They have made my stay at Karlsruhe most instructive and pleasant. The following persons I wish to mention by name: Dr. H. Küsters for the providing of the theme of this study and for his interest for the progress of it, D.P. K. Schroeter for the many valuable discussions and advices and for reading of the manuscript, Dr. J.J. Schmidt for his helpful advices and assistance during the evaluation of the data uncertainties of the reactor materials, Mr. H. Bachmann for the programming of some special codes for this study, Dr. W. Frisch for placing at my disposal a preliminary manuscript of his thesis and for the valuable discussions of the stability of the D-1 design, Dr. K. Hornyik for the valuable discussions of the dynamic behaviour problems and for the calculation of some significant cases with his computer programs.

Last but not least I wish to thank Mrs. U. Besch and Mrs. U. Schwarzlantner for the typing of the manuscript and Miss B. Betsche for the drawing of the figures.

List of Figures

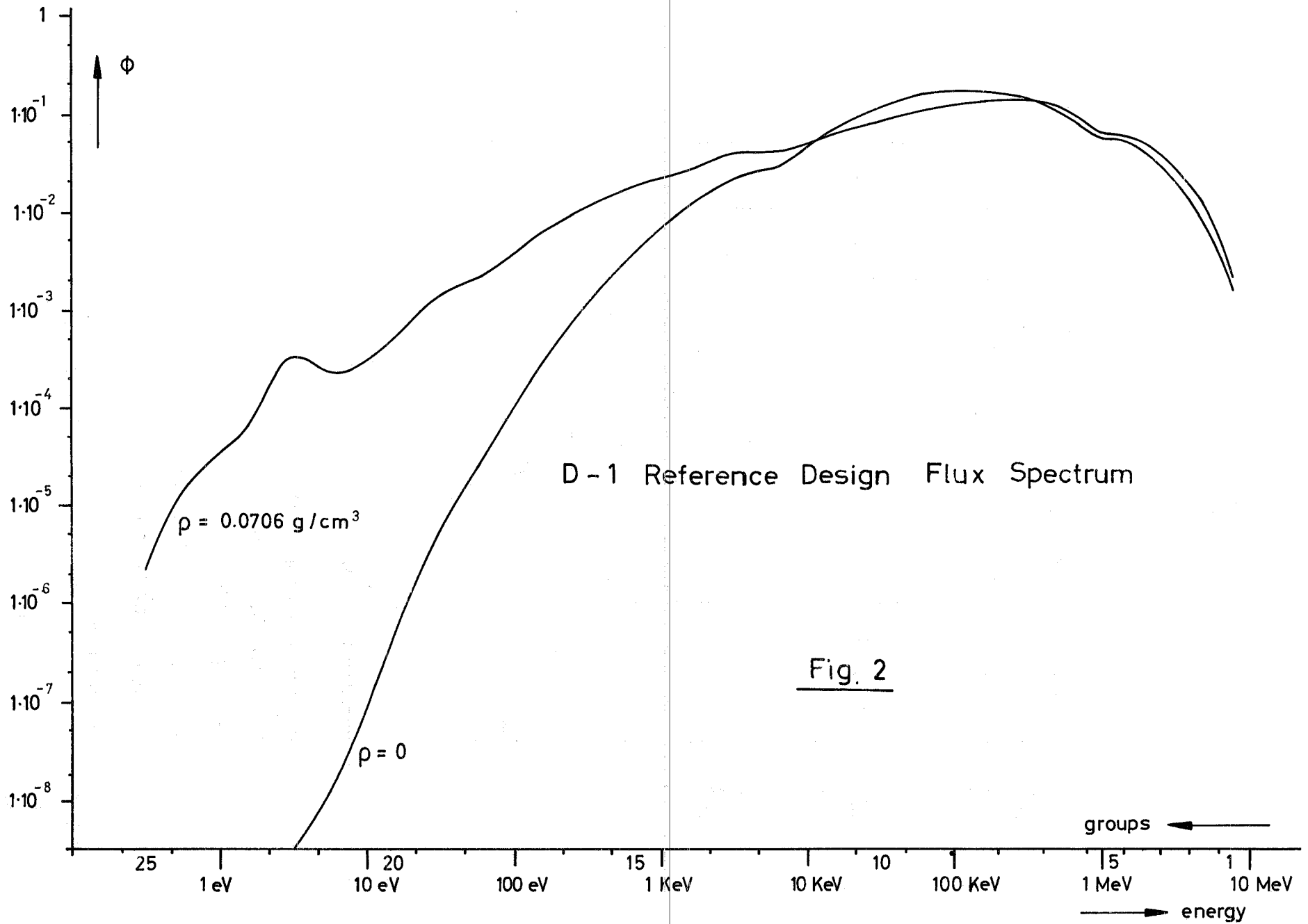
- Fig. 1 Core arrangement for the D-1 design
- Fig. 2 Group flux spectrum of the D-1 design
- Fig. 3 Capture rates of the structural materials
- Fig. 4 Capture rates of the fuel materials
- Fig. 5 Fission rates of the fuel materials
- Fig. 6 Spectral distribution of the Doppler Effect
- Fig. 7 Spectral distribution of the R.S.D.C.
- Fig. 8 Comparison of the flux spectra of the D-1 design and the lattice of Ref. 24
- Fig. 9 The uncertainties of $\alpha = \frac{\sigma_{\gamma}}{\sigma_{\text{f}}}$ of Pu²³⁹
- Fig. 10 Some evaluations of the nuclear data of Pu²⁴⁰
- Fig. 11 Energy dependence of $\frac{\delta\Sigma_{\text{rem}}}{\Sigma_{\text{rem}}} / \frac{\partial y}{y}$
- Fig. 12 Energy dependence of η and adjoint flux
-
- Fig. 13 Influence of the data uncertainties on the stability of the D-1 core
- Fig. 14 Behaviour of the core after a main pipe rupture near the reactor inlet
- Fig. 15 Influence of the reactor parameters on the core temperatures after pipe rupture
- Fig. 16 Influence of the reactor parameters on the thermal power of the core after pipe rupture
- Fig. 17 Influence of the reactor parameters on the total feedback reactivity after pipe rupture
- Fig. 18 Reactivity effects after main pipe rupture with unfavourable D.C. and R.S.D.C. (with and without scram)
- Fig. 19 Fuel and can temperatures after pipe rupture with unfavourable D.C. and R.S.D.C. (with and without scram)

Fig. 1



measures in cm

- a) inner fission region
- b) outer fission region
- c) radial blanket
- d) lower axial blanket
- e) upper axial blanket
- f) gasplenum



D-1 Reference Design Flux Spectrum

Fig. 2

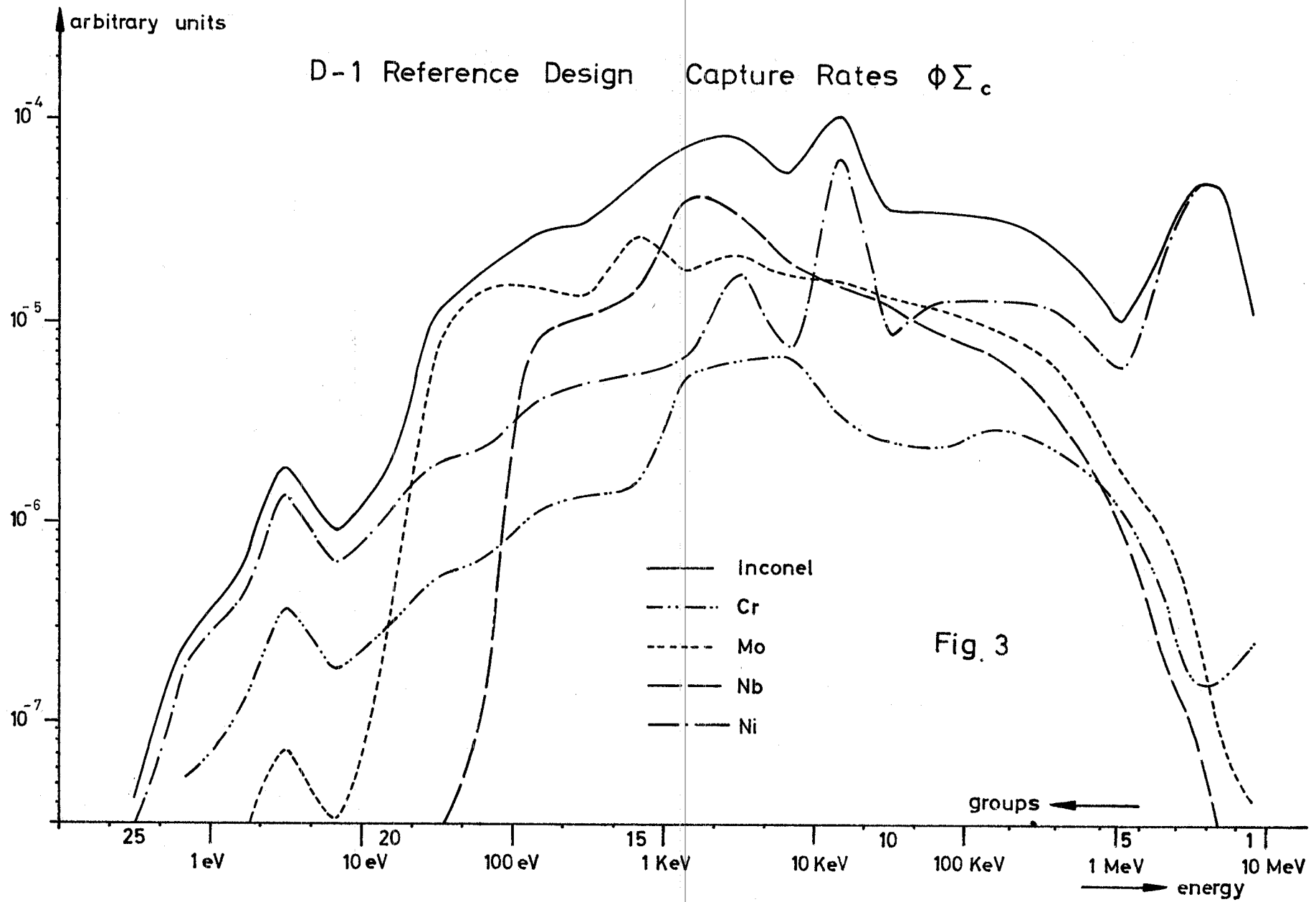
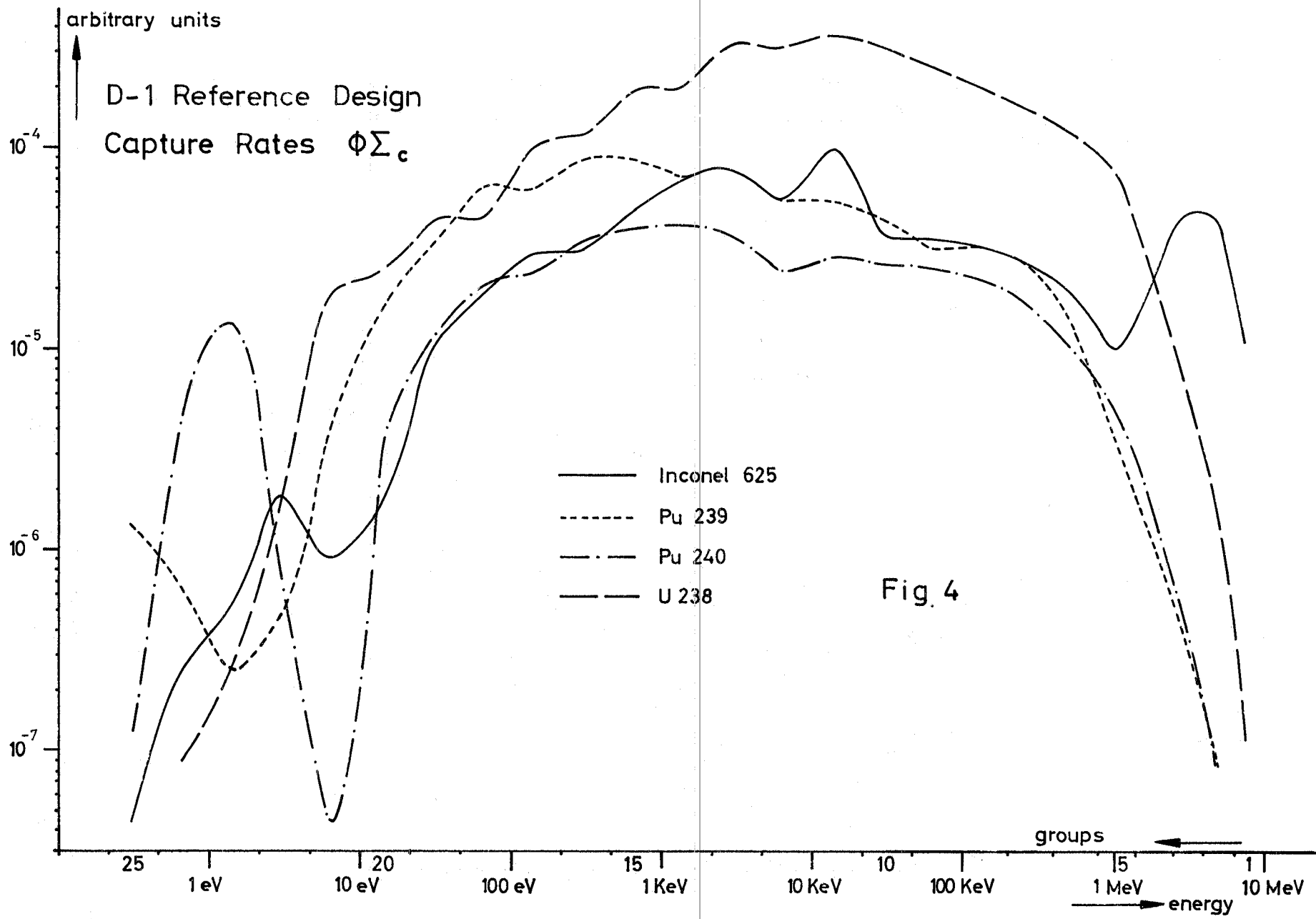
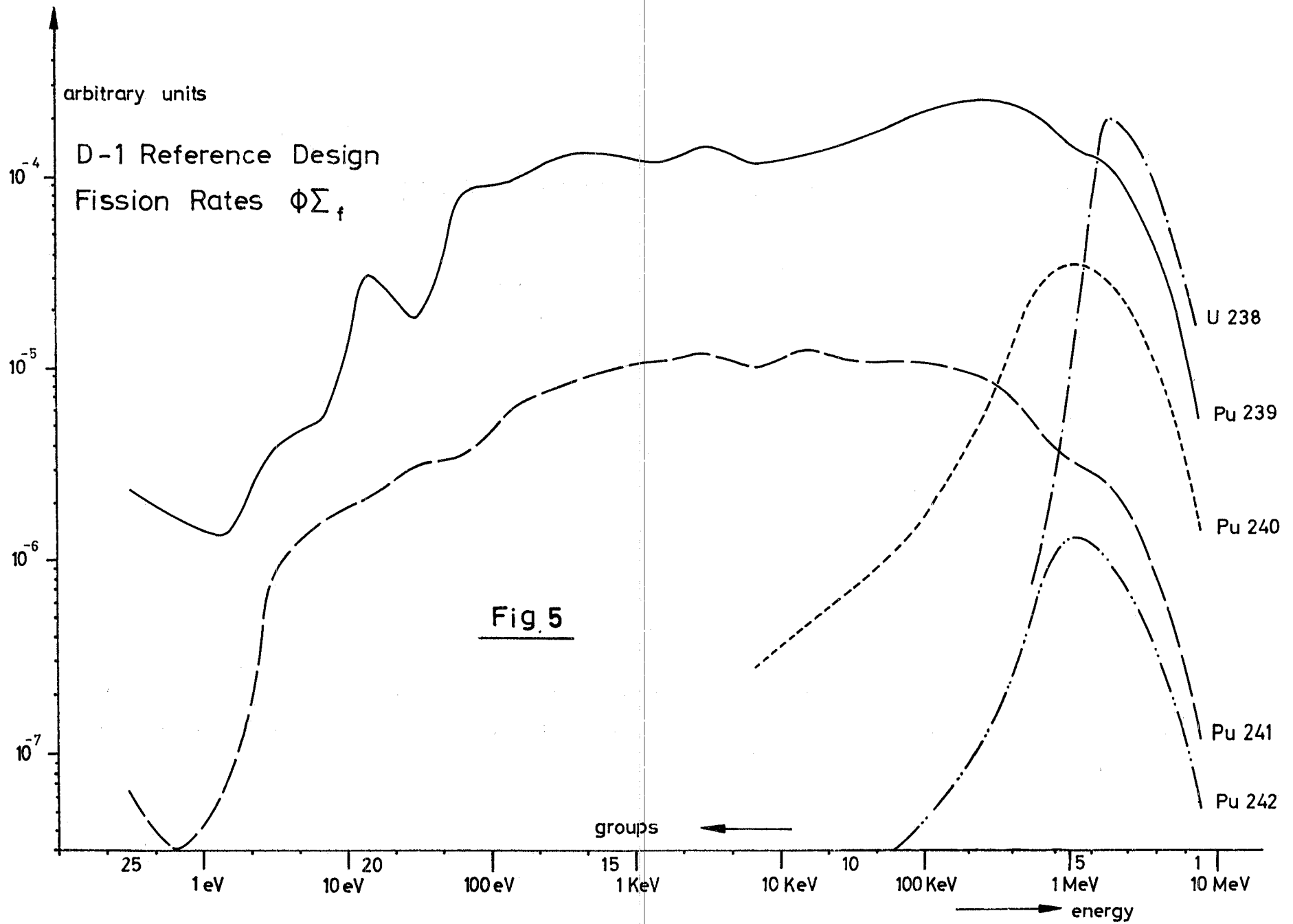
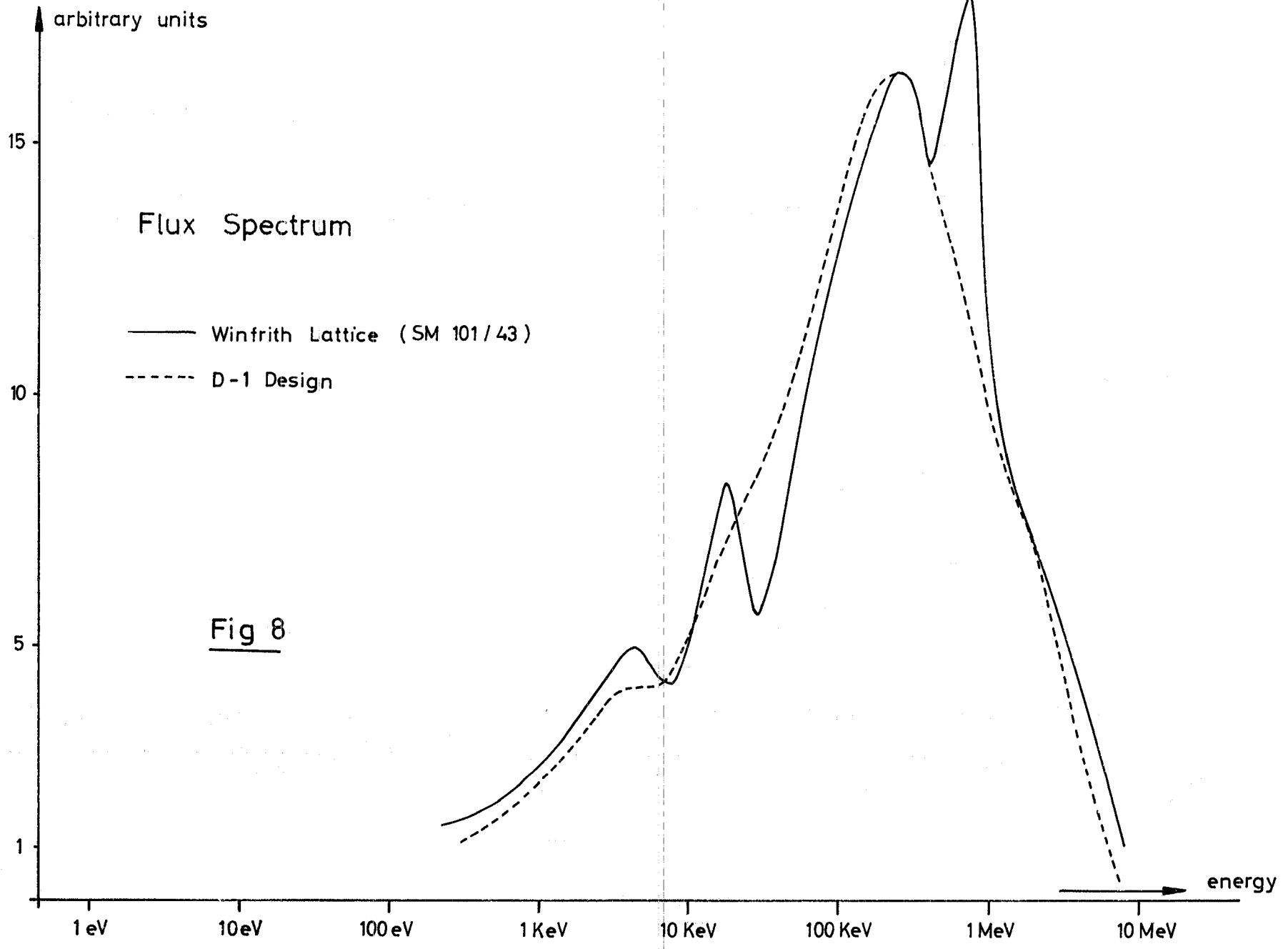
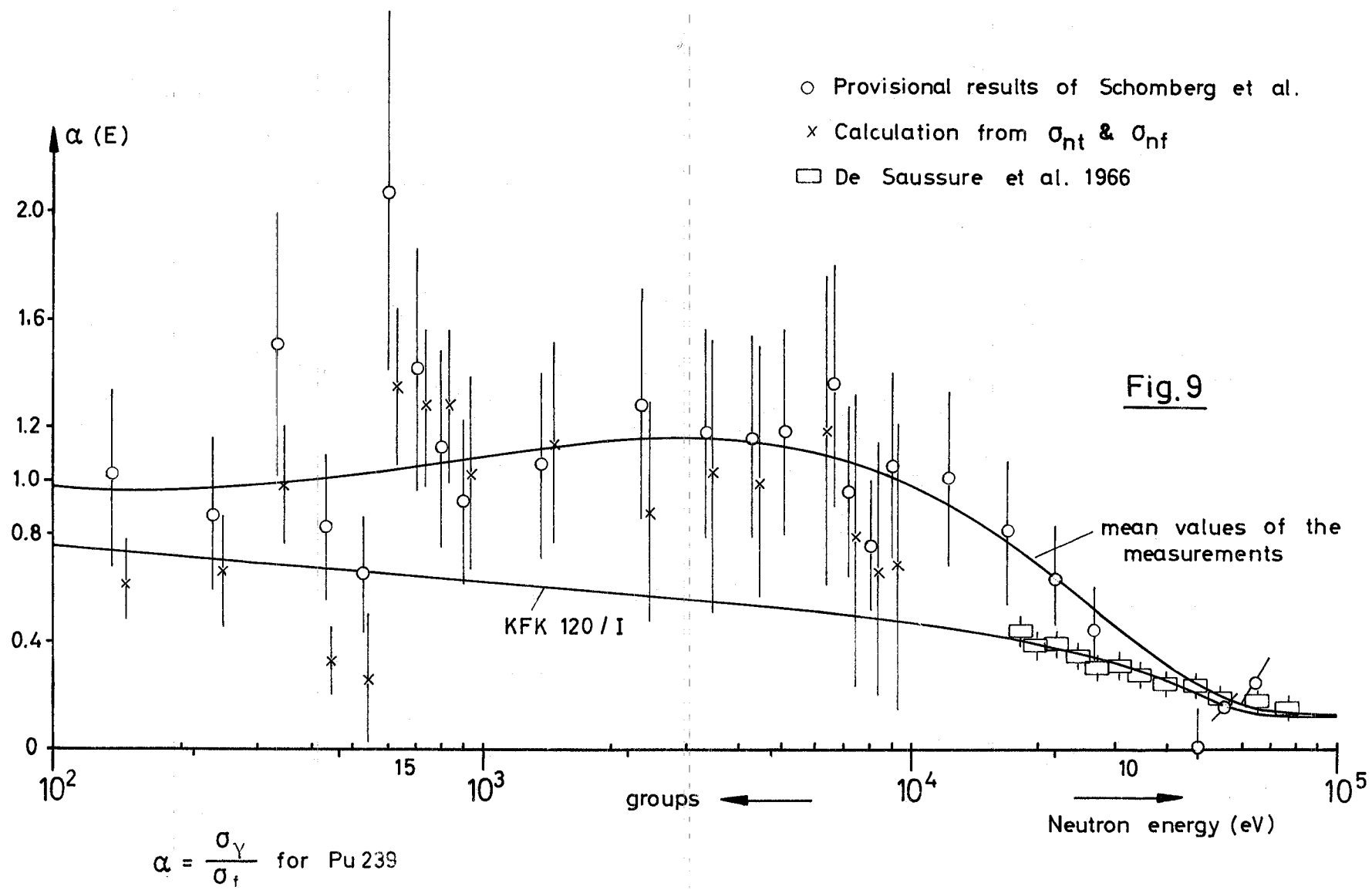


Fig. 3









Fission and Capture Cross Section of Pu 240

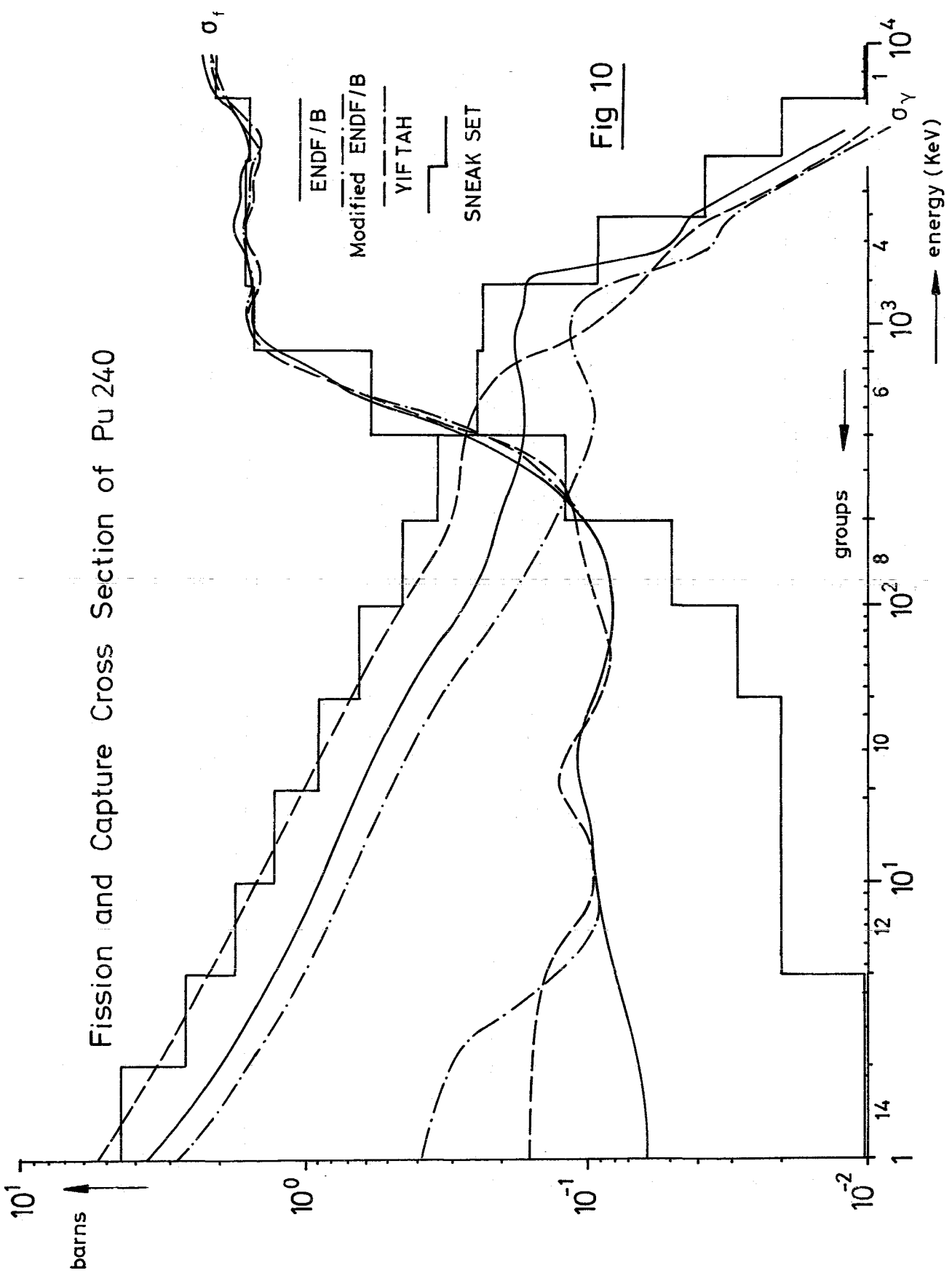


Fig 10

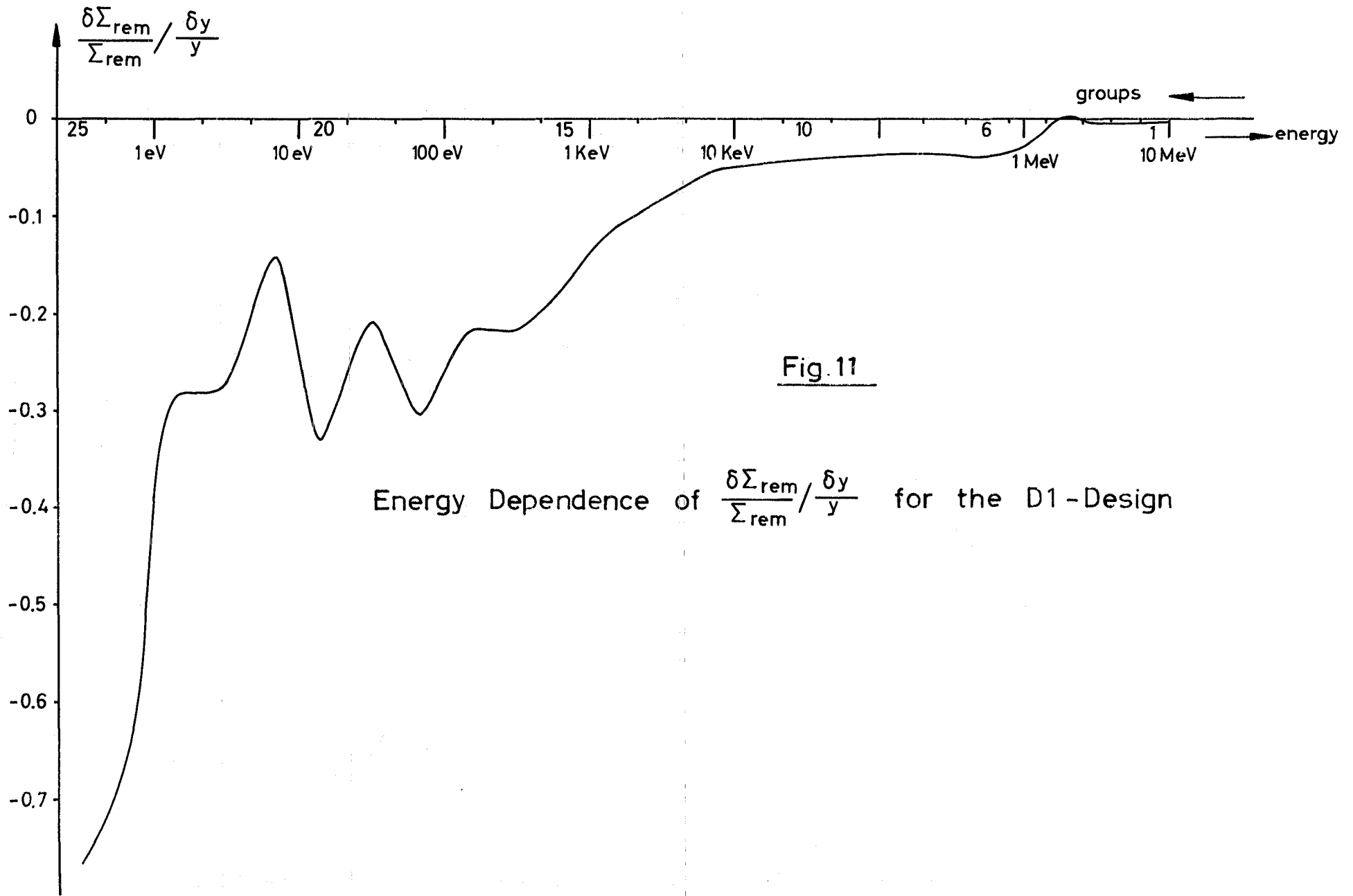
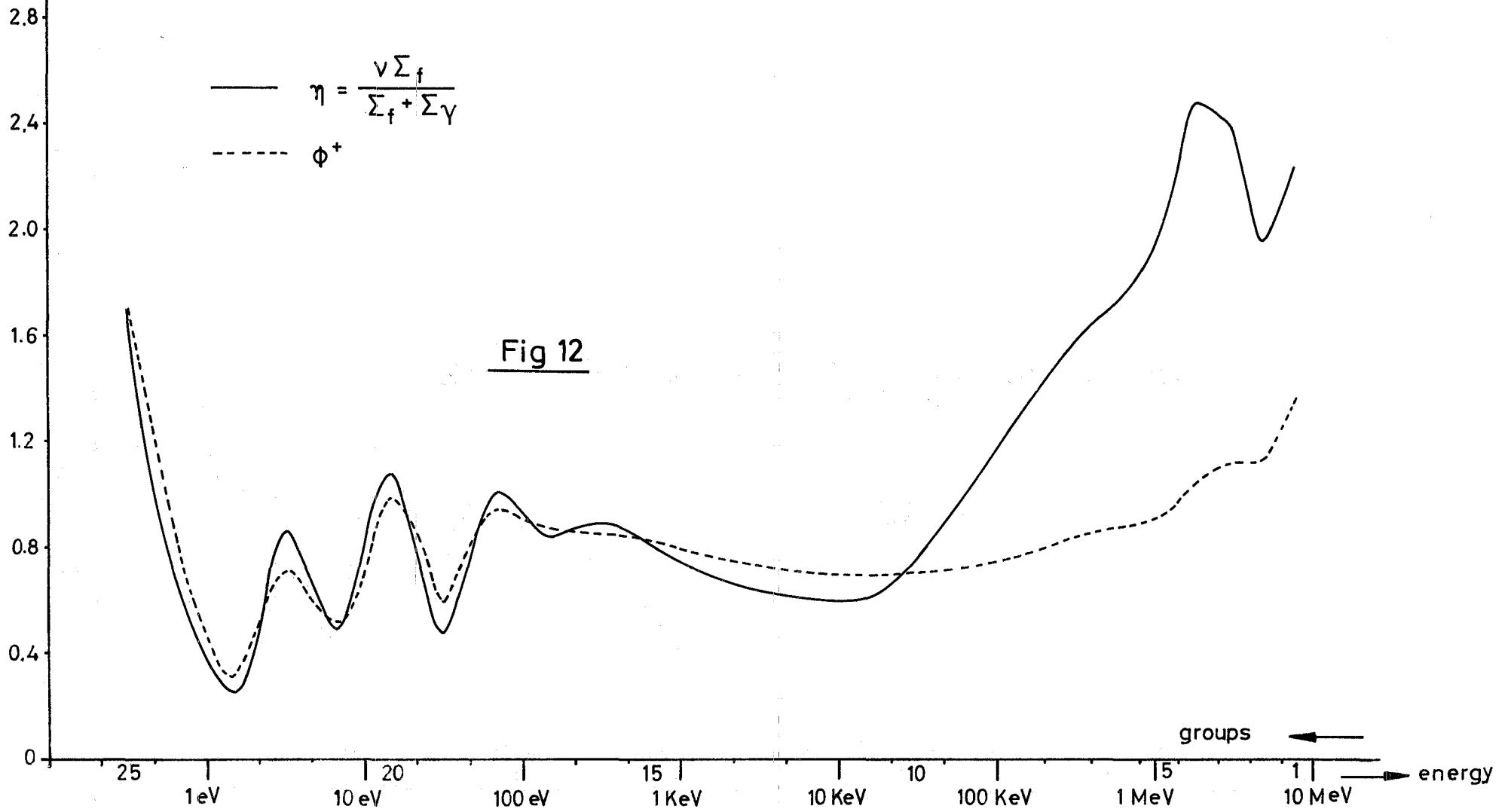
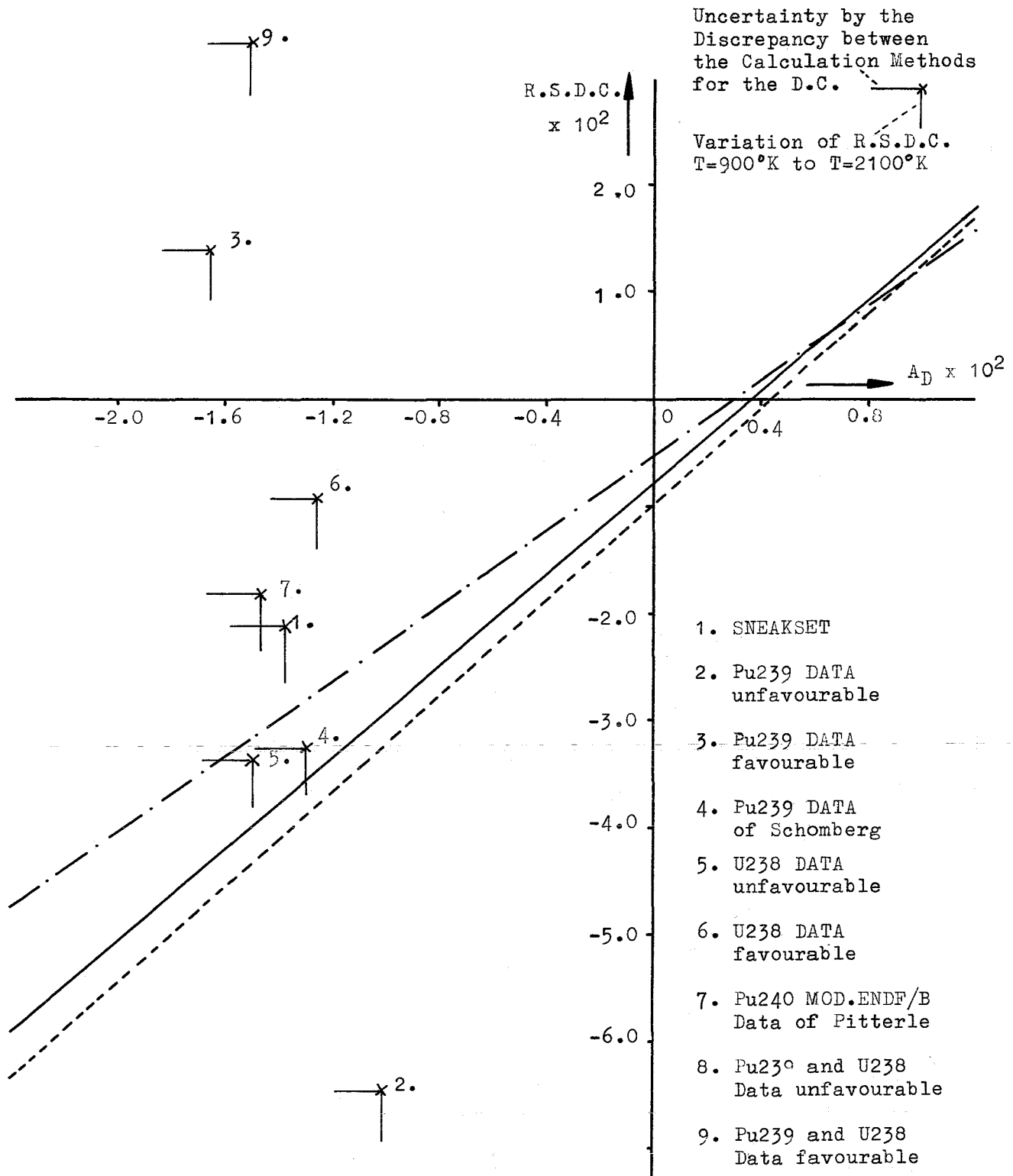


Fig. 11

Energy Dependence of $\frac{\delta \Sigma_{rem}}{\Sigma_{rem}} / \frac{\delta y}{y}$ for the D1-Design

Energy Dependence of η and ϕ^+ for the D1 - Design



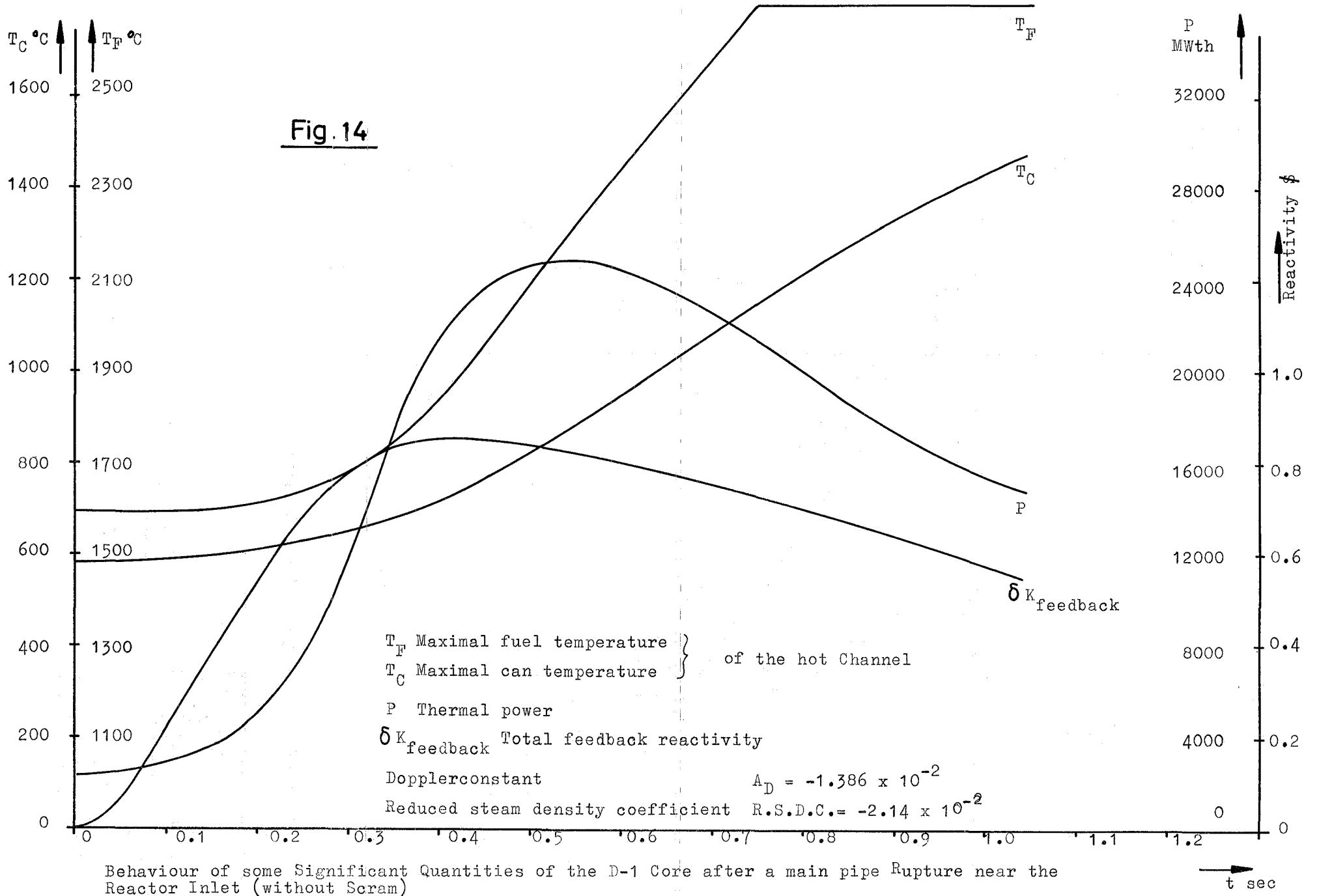


Stable Region above the Curves

	$\frac{\Delta P}{P}$	P/P_n
————	0.01	1
-----	0.75	1
-.-.-.-.	0.01	0.6

Fig. 13

Stability of the D-1 Core



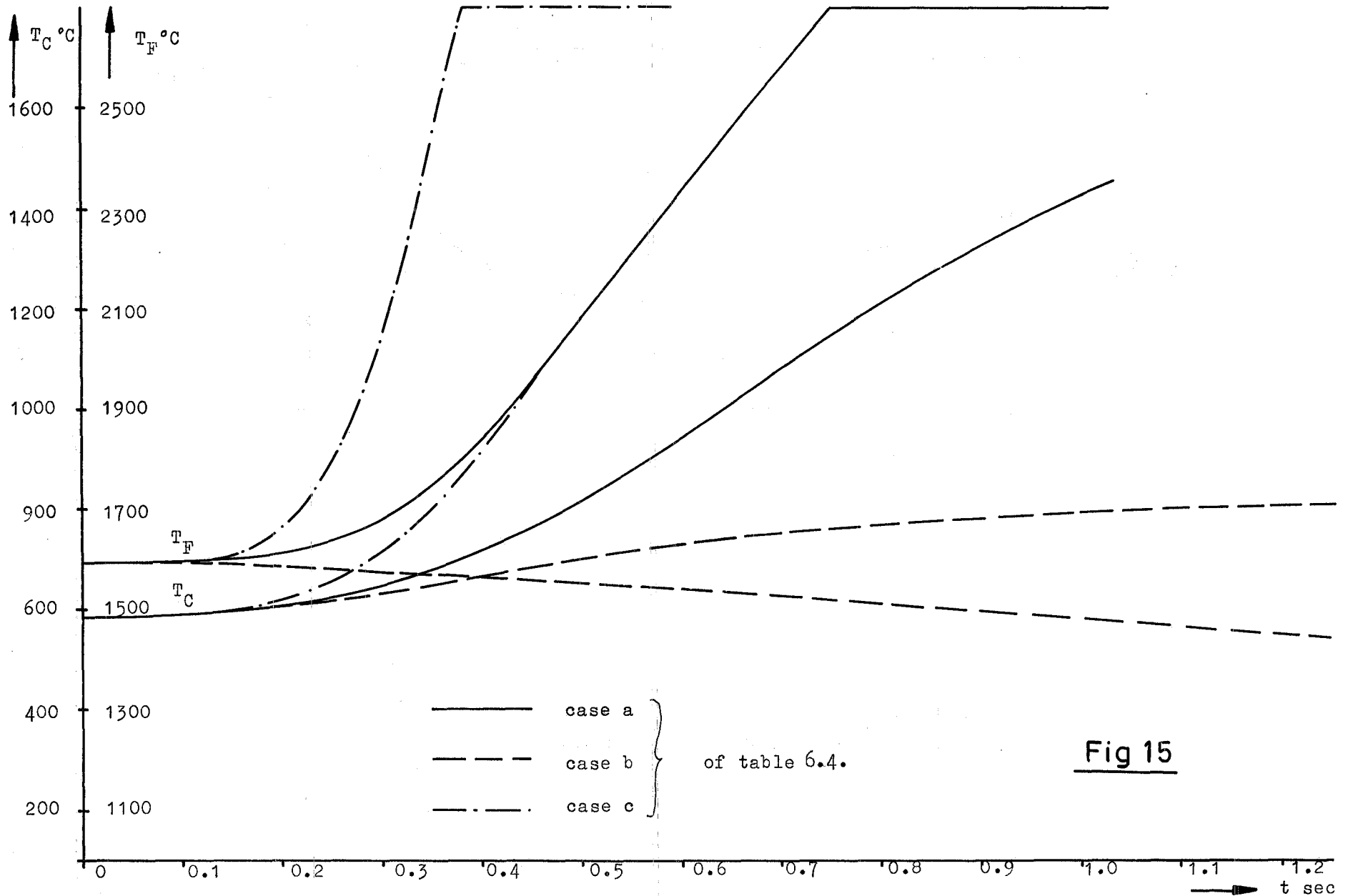
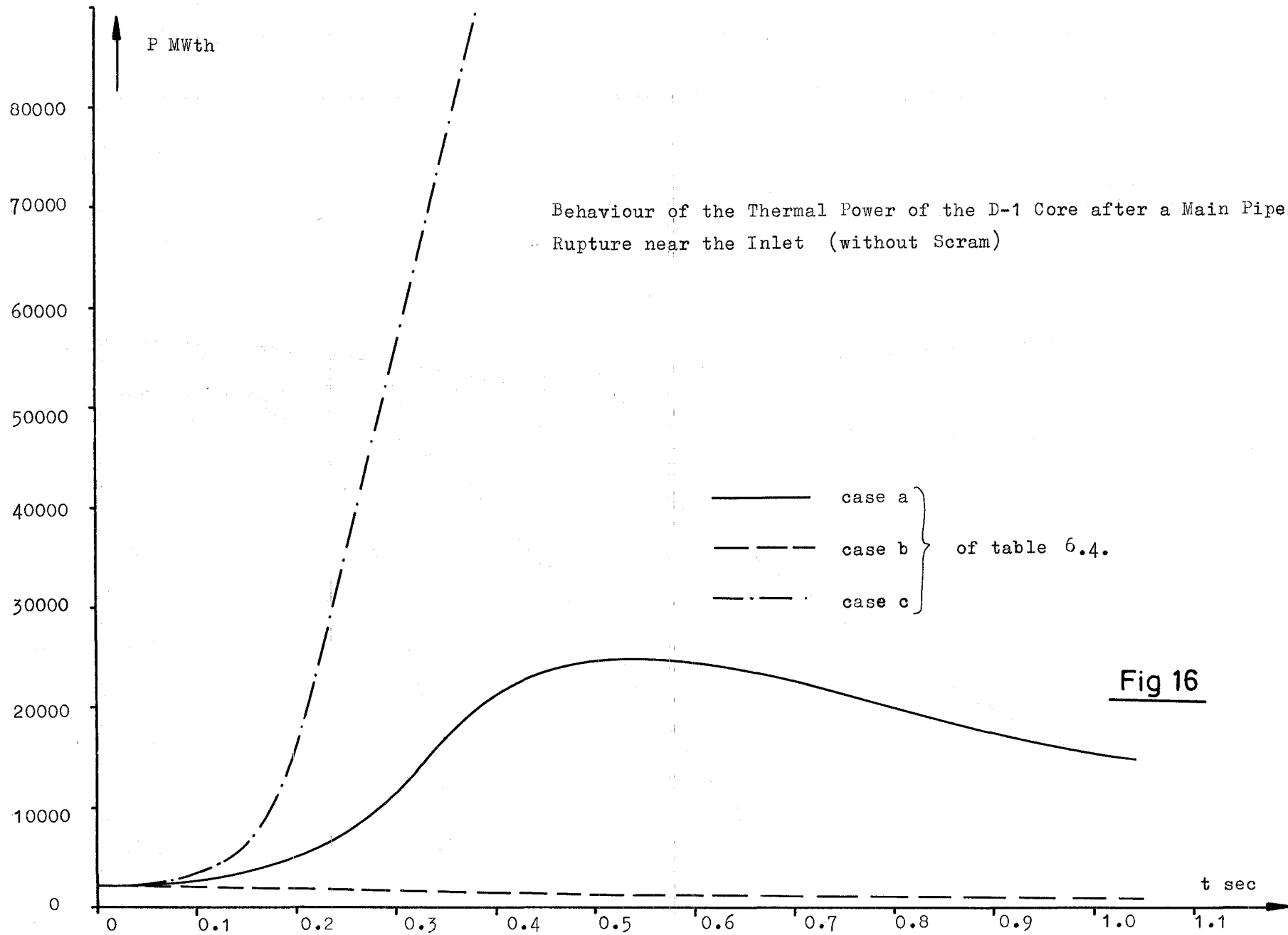


Fig 15

of table 6.4.

The Maximal Fuel and Can Temperature in the Hot Channel after a Main Pipe Rupture near the Reactor Inlet (Without Scram)



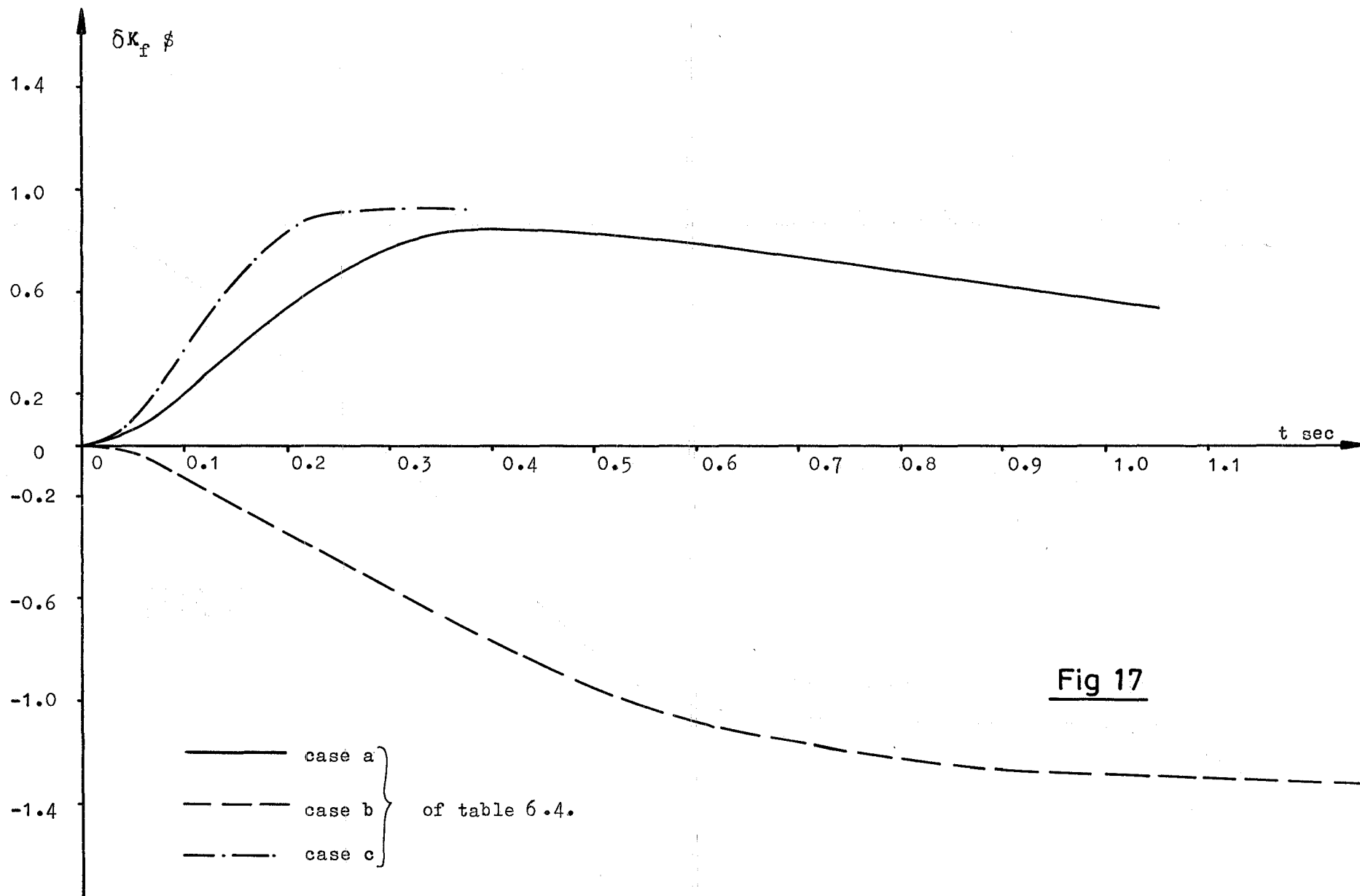
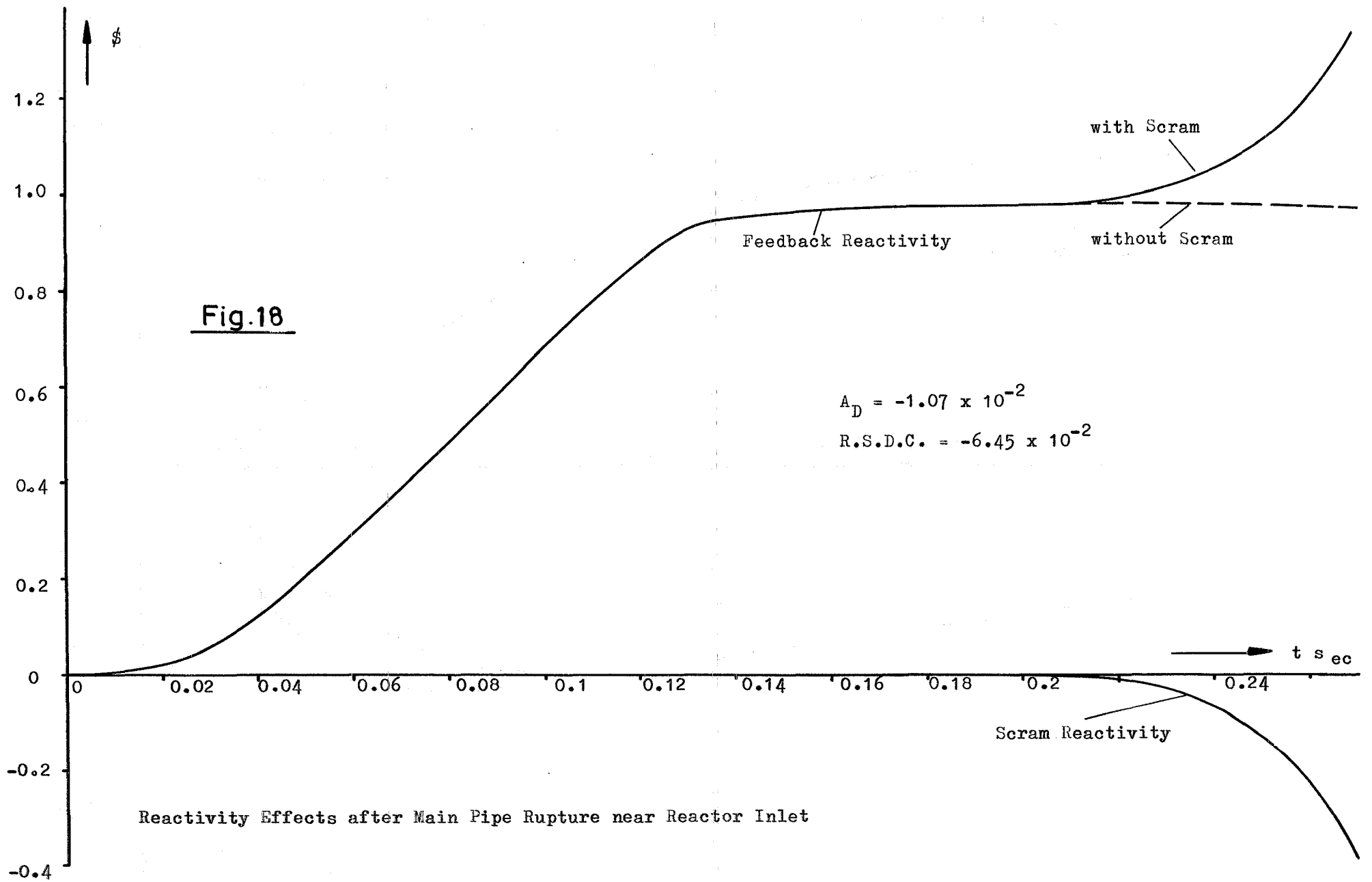
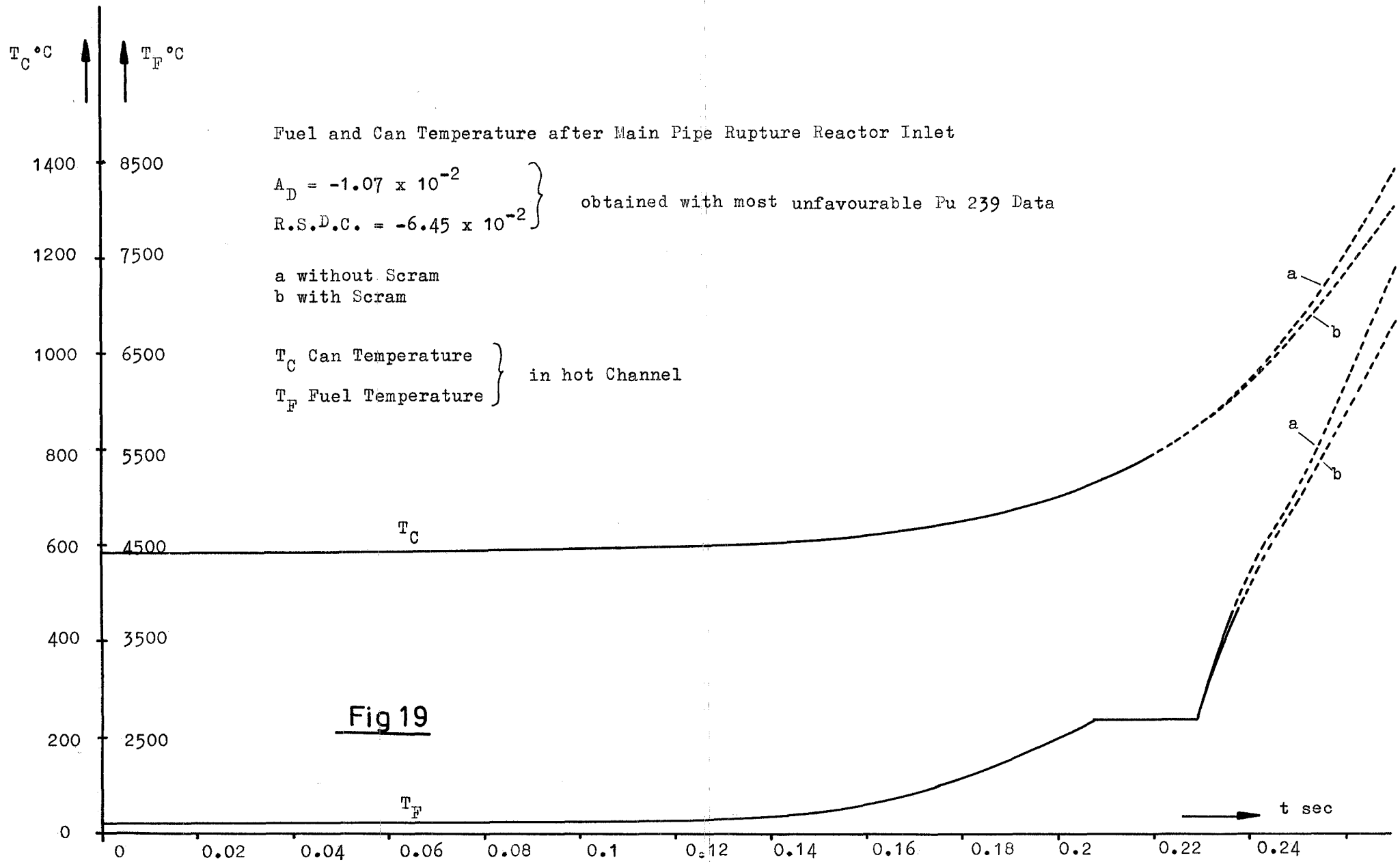


Fig 17

The Total Feedback Reactivity of the D-1 Core after a Main Pipe Rupture near the Reactor Inlet
(Without Scram)





References

- [1] A. Müller et al.
Referenzstudie für den 1000 MWe dampfgekühlten schnellen Brutreaktor (D1)
KFK-Report 392 (1966), Kernforschungszentrum Karlsruhe
- [2] R.A. Müller, F. Hoffmann, E. Kiefhaber, D. Smidt
Design and evaluation of a steam-cooled fast breeder reactor of 1000 MWe
Proceedings of the London Conference on Fast Breeder Reactors, 1966
- [3] A. Jansen
The long-time behaviour of fast power reactors with Pu-recycling
Proceedings of the IAEA Symposium on Fast Reactor Physics and Related Safety Problems, Karlsruhe, 1967
SM 101/16; KFK 630, Eur 3674e
- [4] A. Jansen
Das Langzeitverhalten schneller Reaktoren mit Plutonium-rückführung (Thesis T.H. Karlsruhe)
External report No. INR-4/67-12 (1967), Kernforschungszentrum Karlsruhe
- [5] D. Braess, R. Froelich, A. Jansen, H. Küsters, K. Schroeter
The calculation of large fast reactors
KFK-Report 620 (1967), Kernforschungszentrum Karlsruhe
- [6] H. Bachmann et al.
The group cross-section set KFK-SNEAK, Preparation and results, Proceedings of the IAEA Symposium on Fast Reactor Physics and Related Safety Problems, Karlsruhe, 1967
SM 101/12; KFK 628; Eur 3672e
- [7] H. Huschke
Gruppenkonstanten für dampf- und natriumgekühlte schnelle Reaktoren in einer 26-Gruppendarstellung
KFK-Report 770, Eur 3953d (1968), Kernforschungszentrum Karlsruhe
- [8] L.P. Abagjan et al.
Gruppenkonstanten schneller und intermediärer Neutronen für die Berechnung von Kernreaktoren
KFK-tr-144, Kernforschungszentrum Karlsruhe
- [9] J.J. Schmidt
Influence of nuclear data uncertainties on the theoretical prediction of Doppler coefficients in fast and intermediate reactors
EANDC-46 L (1963)
- [10] H. Bachmann et al.
private communication

- [11] R.B. Nicholson
The Doppler effect in fast nuclear reactors. (Thesis
Cornell University)
APDA 139 (1960)
- [12] R. Froelich
Theorie der Dopplerkoeffizienten schneller Reaktoren
unter Berücksichtigung der gegenseitigen Abschirmung
der Resonanzen
KFK-Report 367 (1964), Kernforschungszentrum Karlsruhe
- [13] R. Froelich and I. Siep
private communication
- [14] P. Greebler et al.
Calculated nuclear reactor parameters and their uncertainties
in a 1000 MWe fast ceramic reactor
GEAP 4471 and ANL 7120 (1965)
- [15] P. Greebler and B. Hutchins
User requirements for cross-sections in the energy range
from 1000 eV to 100 keV
GEAP 4472 (1966)
- [16] J.J. Schmidt
Neutron cross-sections for fast reactor materials
KFK-Report 120, part I, ed. 1966
- [17] J. Stehn et al.
Neutron cross-sections Vol. II-B and III
BNL 325, sec. ed., suppl. 2 (1965)
- [18] S. Yiftah, J.J. Schmidt, M. Caner, and M. Segev
Basic nuclear data for the higher Pu-isotopes
Proceedings of the IAEA Symposium on Fast Reactor
Physics and Related Safety Problems, Karlsruhe, 1967
SM 101/21
- [19] T.A. Pitterle and M. Yamamoto
A comparison of Pu²⁴⁰ cross-section evaluations by
calculations of ZPR III assemblies 48, 48B
Second Conference on Neutron Cross-Sections Technology,
Washington (1968), Paper H 8
- [20] W.G. Schomberg et al.
A new method of method of measuring $\alpha(E)$ for Pu²³⁹
Proceedings of the IAEA Symposium on Fast Reactor Physics
and Related Safety Problems, Karlsruhe, 1967
SM 101/41

- [21] K.H. Beckurts and J.J. Schmidt
private communication
- [22] P.H. White et al.
Measurement of fission cross-sections for neutrons of energy in the range 40-500 keV
Proceedings of the IAEA Symposium, Salzburg, 1965
SM 60/14
- [23] W.P. Pönitz et al.
Some new measurements and renormalizations of neutron capture cross-section data in the keV energy range
Proceedings of the IAEA Symposium on Fast Reactor Physics and Related Safety Problems, Karlsruhe, 1967
SM 101/9; KFK 635; Eur 3679e
- [24] M.J. Arnold, W.N. Fox, C.F. George, R. Richmond
A comparison of experiment with prediction of the variation of k_{∞} with coolant density for a Pu-fueled steam-cooled fast reactor lattice
Proceedings of the IAEA Symposium on Fast Reactor Physics and Related Safety Problems, Karlsruhe, 1967
SM 101/43
- [25] E. Kiefhaber
Konfiguration und nukleare Kenngrößen eines Dampfgekühlten Schnellen Brutreaktors. (Thesis T.H. Karlsruhe)
External report INR-4/67-13 (1967), Kernforschungszentrum Karlsruhe
- [26] K. Jirlow
Reactivity dependence of coolant density in steam-cooled fast reactors
Proceedings of the IAEA Symposium on Fast Reactor Physics and Related Safety Problems, Karlsruhe, 1967, SM 101/52
- [27] W.G. Davey
An analysis of the fission cross-sections of Th-232, U-233, U-234, U-235, U-236, Np-237, U-238, Pu-239, Pu-240, Pu-241, Pu-242 from 1 keV to 10 MeV
Nucl. Sci. Eng., Vol 26 (1966)
- [28] R. Hakansson
private communication
- [29] W. Frisch
Stabilitätsprobleme bei dampfgekühlten schnellen Reaktoren
KFK-Report 759 (1968), Kernforschungszentrum Karlsruhe
- [30] W. Frisch et al.
Safety aspects of steam-cooled fast breeder reactors
KFK-Report 613 (1967), Kernforschungszentrum Karlsruhe

- [31] W. Frisch and E. Schönfeld
Rechenprogramme für Dynamik und Stabilität eines schnellen Leistungsreaktors
KFK-Report 465 (1966), Kernforschungszentrum Karlsruhe
- [32] W. Frisch et al.
Systems analysis of a fast steam-cooled reactor of 1000 MWe
Proceedings of the IAEA Symposium on Fast Reactor Physics and Related Safety Problems, Karlsruhe, 1967
SM 101/10; KFK 636; Eur 3680e
- [33] F. Erbacher et al.
Parametric study of the dynamic behaviour and stability of a steam-cooled fast reactor with an integrated coolant cycle.
Proceedings of the IAEA Symposium on Fast Reactor Physics and Related Safety Problems, Karlsruhe, 1967
SM 101/18; KFK 637; Eur 3681e
- [34] W. Frisch and G. Woite
Analoges Rechenmodell für dampfgekühlte schnelle Reaktoren mit Direktkreislauf
KFK-Report 657, Eur 3693d (1967), Kernforschungszentrum Karlsruhe
- [35] L. Krebs
Die Stabilität von starr zurückgeführten Regelstrecken ohne Ausgleich am Beispiel des dampfgekühlten Reaktors
KFK-Report 656, Eur 3691d (1967), Kernforschungszentrum Karlsruhe
- [36] K. Hornyik
Models, Methods and digital Computer Programs for Analyses in Reactor Dynamics with Emphasis on Fast Breeder Reactors and Compressible Single-Phase Coolants
KFK-Report 799, Eur 3964d (1968), Kernforschungszentrum Karlsruhe
- [37] K. Thurnay
private communication